BIOLOGICAL SCIENCES: Immunology and Inflammation

Akt signaling is critical for memory CD8$^+$ T cell development and tumor immune surveillance

Anne Rogel, Jane E. Willoughby, Sarah L. Buchan, Henry J. Leonard, Stephen M. Thirdborough and Aymen Al-Shamkhani[1]

Cancer Sciences, Faculty of Medicine, University of Southampton, Southampton General Hospital, Tremona Road, Southampton SO16 6YD, UK.

Correspondence should be addressed to: Aymen Al-Shamkhani

Email: aymen@soton.ac.uk.

Tel: 0044 23 81206285

Running title: Akt signaling is required for memory CD8$^+$ T cells

Abstract

Memory $CD8^+$ T cells confer long-term immunity against tumors and anti-cancer vaccines should therefore maximize their generation. Multiple memory $CD8^+$ T cell subsets with distinct functional and homing characteristics exist, yet the signaling pathways that regulate their development are ill defined. Here we examined the role of the serine/threonine kinase Akt in the generation of protective immunity by $CD8^+$ T cells. Akt is known to be activated by the T cell antigen receptor and the cytokine IL-2, but its role in T cell immunity *in vivo* has not been explored. Using $CD8^+$ T cells from *pdk1*$^{K465E/K465E}$ knockin mice we found that decreased Akt activity inhibited the survival of T cells during the effector to memory cell transition and abolished their differentiation into $CXCR3^{lo}CD43^{lo}$ effector-like memory cells. Consequently, anti-tumor immunity by $CD8^+$ T cells that display defective Akt signaling was substantially diminished during the memory phase. Reduced memory T cell survival and altered memory cell differentiation were associated with upregulation of the pro-apoptotic protein Bim and the T-box transcription factor eomesodermin, respectively. These findings suggest an important role for effector-like memory $CD8^+$ T cells in tumor immune surveillance and identify Akt as a key signaling node in development of protective memory $CD8^+$ T cell responses.

Significance Statement

Immunotherapy has emerged as an important modality for the treatment of cancer and T cell vaccination provides an opportunity to generate long lasting anti-cancer responses. Critical to this is the generation of memory $CD8^+$ T cells, yet the signaling pathways that regulate their development are incompletely defined. In the current report we have focused on the serine/threonine protein kinase Akt. Although Akt is known to be activated by the T cell antigen receptor and the cytokine IL-2, its role in T cell immunity remains unknown. In this study we show that Akt signaling profoundly impacts on memory T cell development and the anti-tumor response during the memory phase. Optimizing Akt activity should therefore maximize the therapeutic effect of anti-cancer vaccines.

"\Body"

In a typical immune response to an acute infection, naive $CD8^+$ T cells expand and differentiate into effector cells that target infected cells for destruction. Following elimination of the pathogen, the majority (90-95%) of effector cells die by apoptosis while the remaining cells mature into memory cells. The mechanisms that regulate memory $CD8^+$ T cell generation are not fully defined. However, several lines of evidence indicate that increasing the intensity of inflammation skews differentiation towards short-lived effector cells (SLECs) at the expense of memory precursor effector cells (MPECs) (1-4). The memory $CD8^+$ T cell pool consists of populations of cells that vary in a number of characteristics, including tissue trafficking, effector function and recall responses. Initially two memory cell subsets were identified based on expression of CD62L and CCR7 (5-7). Thus, central memory T cells (T_{CM}), which express CD62L and CCR7, localize preferentially to lymph nodes (LNs) and exhibit strong recall responses as well as robust IL-2 production. In contrast, effector memory T cells (T_{EM}), which lack CD62L and CCR7, traffic preferentially to non-lymphoid tissues, possess heightened cytotoxicity towards target cells, and display a limited proliferative recall capacity (5-7). More recently, Hikono et al, identified distinct memory $CD8^+$ T cell subsets based on expression of CXCR3, CD27 and an activation-associated glycoform of CD43 (8). These markers further divide circulating T_{CM} and T_{EM} cells into subsets that differ in homeostatic proliferation, persistence, granzyme B expression, production of IL-2 and recall responses. $CD27^{hi}CXCR3^{hi}CD43^{lo}$ memory $CD8^+$ T cells persist for longer and generate better recall responses when compared with $CD27^{lo}CXCR3^{lo}CD43^{lo}$ memory cells, yet the latter subset confer the most efficient protective immunity against infection with *Listeria monocytogenes* or vaccinia virus (9).

The signaling pathways that regulate the development of memory T cell subsets are not well understood, yet knowledge of these pathways is important for the development of more efficacious vaccines against tumors and intracellular pathogens. In the current report we

have focused on the serine/threonine protein kinase Akt. Akt regulates nutrient uptake and cellular metabolism in many cell types, but appears to be dispensable for these processes in mature $CD8^+$ T cells (10). Akt regulates the T cell receptor (TCR) and IL-2 transcriptional programs that control the expression of cytolytic molecules, adhesion receptors and cytokine and chemokine receptors that distinguish effector from naive and memory cells (11, 12). It has therefore been suggested that Akt activity promotes the differentiation of naive $CD8^+$ T cells into cytotoxic T cells at the expense of memory cells (11, 12). However, this view is based on findings derived from *in vitro* studies and therefore the true impact of physiological Akt activation on $CD8^+$ T responses *in vivo* remains unknown. A critical step for Akt activation is the phosphorylation of Thr308 by phosphoinositide-dependent kinase 1 (PDK1). This event is mediated by the tethering of Akt and PDK1 to the plasma membrane via their pleckstrin homology (PH) domains (13). The PH domains of Akt and PDK1 bind to the lipid second messenger phosphatidylinositol 3,4,5-trisphosphate (PIP_3), the product of the class I phosphatidylinositol 3-kinases (PI3Ks). Hence, knock-in mice that express a mutant form of PDK1 (PDK1-K465E) which cannot bind to PIP3 have strongly reduced Akt activation, whilst other PDK1 targets remain unaffected (13, 14). Since low levels of Akt activity remain in PDK1-K465E mice, thymic development of T cells, which is absent in Akt knockout mice (15), proceeds normally (14). Thus, PDK1-K465E knock-in mice provide a powerful model to investigate the role of Akt signaling in mature T cells. Using $CD8^+$ T cells from PDK1-K465E knock-in mice we now show that, contrary to the currently held view, Akt signaling is critical for $CD8^+$ memory T cell development.

Results

Reduced Akt signaling does not impede the generation of primary effectors. Analysis of TCR-mediated phosphorylation of Akt at Thr308 in PDK1-K465E and PDK1-WT cytotoxic T cells (CTLs) confirmed the reduced ability of PDK1-K465E OT-I cells to activate Akt (Fig. S1A). In addition, mTORC1 activity, as assessed by the levels of phospho-S6 at Ser235/236, was still detectable in PDK1-K465E CTLs (Fig. S1B), consistent with previous findings demonstrating that mTORC1 activation in $CD8^+$ T cells can be induced independently of Akt activation (16). Next we investigated the effect of reduced Akt signaling on the $CD8^+$ T cell response following vaccination with ovalbumin (OVA) protein, co-administered with agonist anti-CD40 mAb and LPS. This vaccination approach induces robust expansion of cytotoxic effectors, and long-lived lymphoid and mucosal memory $CD8^+$ T cells (17, 18). We adoptively transferred a small number of PDK1-K465E or PDK1-WT OT-I cells, which bear a TCR specific for the $OVA_{257-264}$/H-$2K^b$ complex, into C57BL/6 mice prior to vaccination. At the peak of the response similar numbers of PDK1-WT and PDK1-K465E donor OT-I cells were recovered from the spleen, LNs and blood, indicating that maximal Akt activation is not required for the expansion of $CD8^+$ T cells *in vivo* (Fig. 1A). The impact of reduced Akt activity on OT-I T cell effector function was also minimal with a small but reproducible decrease in the proportion of granzyme B^+ cells in the PDK1-K465E OT-I population compared to PDK1-WT effectors (Fig. 1B). Furthermore, frequencies of IFN-γ and TNF-α-producing cells were similar among PDK1-WT and PDK1-K465E OT-I effectors, whereas the proportion of cells that produced IL-2 was marginally higher among PDK1-K465E effectors (Fig. 1C and Fig. S1C). Moreover, cytokine production on a per cell basis was indistinguishable between the two cell types (Fig. S1D). Similar results were obtained when the anti-CD40/LPS adjuvant was replaced with agonist anti-4-1BB mAb/LPS or polyI:C (Fig. S1E-H). Finally, to determine the broader impact of the PDK1-K465E mutation on effector

function and protective immunity *in vivo*, we compared the ability of PDK1-WT and PDK1-K465E OT-I T cells to control the growth of OVA-expressing E.G7 tumor cells. Four days after E.G7 inoculation, mice received either naive PDK1-WT or PDK1-K465E OT-I T cells followed by OVA/anti-CD40/LPS. As shown in Fig. 1D, PDK1-K465E and PDK1-WT OT-I cells were equally effective in controlling tumor growth. Thus, collectively, our data demonstrate that the development of primary effectors following protein vaccination is largely insensitive to sub-optimal Akt activity.

Generation of memory CD8$^+$ T cells following protein vaccination requires Akt signaling. To assess the impact of reduced Akt signaling on the memory CD8$^+$ T cell response, we monitored the contraction of OT-I T cells in blood following vaccination with OVA/anti-CD40/LPS. As shown in Fig. 2A, PDK1-K465E OT-I cells displayed an accelerated contraction phase compared to PDK1-WT cells. Furthermore, when equal numbers of PDK1-WT and PDK1-K465E OT-I cells were co-transferred into congenic mice, PDK1-WT cells did not rescue the rapid contraction of PDK1-K465E cells, demonstrating a cell-intrinsic defect in the ability of PDK1-K465E cells to transition from the effector to the memory stage (Fig. 2B). Despite reaching similar frequencies at the peak of the primary response, fewer PDK1-K465E OT-I T cells were recovered at the resting memory phase in both lymphoid and non-lymphoid tissues (Fig. 2C). In order to discriminate between tissue-localized and vasculature-associated memory CD8$^+$ T cells, we performed intravascular (i.v.) antibody labelling as described by Anderson et al (19). The majority of CD45.1$^+$CD8$^+$ T cells recovered from the lungs and liver were not protected from i.v. anti-CD8α mAb (Fig. S2A). In contrast, almost all CD45.1$^+$CD8$^+$ T cells isolated from the intestine were protected from i.v. antibody labelling (Fig. S2A). These experiments revealed that reduced Akt signaling had the greatest effect on vasculature-associated memory CD8$^+$ T cells in the lungs and liver (Fig. S2B). Importantly, the reduction in the frequency of i.v. mAb-protected PDK1-K465E OT-I

memory cells in the intestine demonstrated that Akt signaling is required for optimal accumulation of memory cells in the intestine parenchyma, following vaccination with OVA/anti-CD40/LPS (Fig. S2B).

We next determined whether reduced Akt signaling selectively impairs the development of a particular subset of memory cells. This analysis was conducted 6-7 weeks after immunization when PDK1-K465E OT-I cells were still readily detectable. Initially we analyzed the expression of CD62L, a marker classically used to discriminate T_{CM} from T_{EM} (5, 6). The frequency of $CD62L^{hi}$ cells was higher among PDK1-K465E OT-I cells in both the spleen and LNs, suggesting that Akt activity normally restrains generation of T_{CM} (Fig. S2C). However, CD62L is transcriptionally induced by Foxo1, which is inactivated by Akt phosphorylation (14, 20, 21). Thus, the increased expression of CD62L on PDK1-K465E memory cells may not truly reflect their differentiation state. We therefore used a complementary strategy based on expression of CXCR3 and an activation-associated glycoform of CD43 to delineate the various memory T cell subsets (8, 9). In the memory phase, PDK1-WT OT-I cells gave rise to subsets that conformed to previously defined phenotypic features obtained in disparate models, with $CXCR3^{lo}CD43^{lo}$ cells displaying the lowest amount of CD62L and the highest levels of killer cell lectin-like receptor G1 (KLRG1) and granzyme B (Fig. S2D). As depicted in Fig. 2D, the frequency of $CXCR3^{lo}CD43^{lo}$ cells was highest in non-lymphoid organs such as liver and lungs and lowest in LNs. Intravascular staining showed that the $CXCR3^{lo}$ memory cells recovered from the lungs and liver are associated with the vasculature, whereas $CXCR3^{lo}$ memory cells recovered from the intestine are protected from i.v. anti-CD8α mAb and therefore localized in the parenchyma (Fig. S2E). Importantly, the percentage of $CXCR3^{lo}CD43^{lo}$ cells among the PDK1-K465E OT-I population was noticeably reduced and this was associated with a reciprocal increase in the frequency of $CXCR3^{hi}CD43^{lo}$ cells (Fig. 2D). These data indicate that the generation of

CXCR3^{lo}CD43^{lo} effector-like memory cells is particularly sensitive to the reduction in Akt signaling.

To address how the diminution in resting memory cells influenced the recall response, mice were re-challenged with $OVA_{257-264}$. The magnitude of the secondary response was significantly reduced when memory T cells were derived from PDK1-K465E OT-I T cells (Fig. 3A). Additionally, PDK1-K465E secondary effectors expressed less granzyme B compared to PDK1-WT cells (Fig. 3B and Fig. S3A). In the few mice that had detectable memory PDK1-K465E cells the fold-expansion of PDK1-K465E memory cells was similar to that of PDK1-WT cells, indicating that decreased Akt activity affected memory cell generation rather than the cell's capacity to mount a secondary proliferative response (Fig. S3B). To assess if the reduced recall response impacted on immune protection, we inoculated mice with E.G7 tumor cells 3 days after secondary immunization. As shown in Fig. 3C, mice that possessed memory PDK1-WT OT-I cells were better protected than those that had PDK1-K465E OT-I memory T cells. Finally, we showed that reduced Akt signaling abolished memory CD8$^+$ T cell formation in two additional protein vaccines that encompass alternative adjuvants (Fig. S3C and D). These results demonstrate that Akt signaling is required for the effector to memory cell transition after protein/adjuvant vaccination.

Vaccine-induced PDK1-K465E OT-I effectors express increased levels of the pro-apoptotic protein Bim. To probe the mechanism underpinning the diminished ability of PDK1-K465E OT-I effector cells to transition into the memory phase, we first assessed if reduced Akt activity affected the ratio of SLECs to MPECs as defined by differential expression of CD127 and KLRG1 (1). The frequency of CD127^{hi}KLRG1^{lo} cells, defined by this criteria as MPECs, was higher among PDK1-K465E effectors (Fig. 4A and B). However, the use of CD127 to demarcate MPECs in this case is complicated by the fact that *Il7ra* is a

target of Foxo1, a transcription factor inactivated by Akt (20-22). Therefore, the frequency of PDK1-K465E MPECs as identified by CD127 expression may be artificially inflated. This is supported by the observation that PDK1-K465E effectors exhibited higher expression of CD127 on both KLRG1^{hi} and KLRG1^{lo} cells when compared to PDK1-WT cells (Fig. S4).

As Bim-deficient effector CD8$^+$ T cells are largely resistant to apoptosis during the contraction phase (23), we hypothesized that increased Bim protein in PDK1-K465E OT-I effectors accelerates cell death and limits generation of memory cells. Comparing the amount of Bim protein in PDK1-WT and PDK1-K465E OT-I effectors isolated 7 days post-vaccination revealed a two-fold increase in its expression in PDK1-K465E OT-I cells (Fig. 4C). Thus, our findings support the notion that physiological Akt activity in effector T cells exerts pro-survival effects by limiting the expression of the pro-apoptotic protein Bim.

The role of Akt signaling in CD8$^+$ T cell differentiation after infection with *Listeria monocytogenes*. To understand the role of Akt signaling in effector CD8$^+$ T cell differentiation in a more inflammatory setting, we compared the responses of adoptively transferred PDK1-WT and PDK1-K465E OT-I cells following infection with OVA-expressing *Listeria monocytogenes* (Lm-OVA). On day 6 post-infection, the frequency of PDK1-K465E OT-I effectors in the spleen and blood was lower than that of PDK1-WT cells (Fig. 5A). This was not due to reduced proliferation of PDK1-K465E OT-I cells, as the frequency of Ki67$^+$ cells among PDK1-WT and PDK1-K465E effectors in spleen was comparable (Fig. S5A), but instead was due to preferential localization of PDK1-K465E OT-I cells in LNs (Fig. 5A and 5B). CD62L expression was higher on PDK1-K465E OT-I cells (Fig. 5C) and this likely contributed to redirecting their trafficking to LNs. Since reduced Akt activity results in high CD127 expression on both KLRG1^{hi} and KLRG1^{lo} cells (Fig. S5B and C), we used KLRG1 expression alone to identify the various effector cell subsets. Disparate

levels of KLRG1 subdivide the effector cell population into subsets that are enriched in either terminal effectors or precursors of T_{CM} (24). As expected, the frequency of KLRG1^{hi} cells generated after Lm-OVA infection (Fig. 5D and Fig. S5B and D) was greater than following protein vaccination (Fig. 4A) (25). The proportion of KLRG1^{hi} cells was lower in the PDK1-K465E OT-I population in the spleen (Fig. 5D) and blood (Fig. S5B and D) leading to a two-fold reduction in the numbers of PDK1-K465E KLRG1^{hi} cells compared to PDK1-WT KLRG1^{hi} cells (Fig. 5D). Furthermore, although an increase in the proportion of CD127^{hi} cells among PDK1-K465E OT-I effectors was evident in the spleen, the numbers of PDK1-K465E and PDK-WT CD127^{hi} T cells were similar (Fig. 5E).

Next we assessed the effect of reduced Akt signaling on effector function. Consistent with our findings in the protein vaccination setting, PDK1-K465E OT-I exhibited only a modest reduction in granzyme B expression compared to PDK1-WT effectors (Fig. S5E). Mobilisation of the degranulation marker CD107a at the cell surface as well as IFN-γ and TNF-α production were equivalent among PDK1-WT and PDK1-K465E (Fig. S5F-I). Although MPECs and SLECs exhibit equivalent cytotoxicity and a similar capacity to produce TNF-α and IFN-γ, MPECs produce more IL-2 than SLECs (1, 24). We found that the proportion of IL-2-producing cells was significantly higher among PDK1-K465E effectors, while IL-2 production on a per cell basis was equivalent (Fig. 5F and Fig. S5H and I), indicating that PDK1-K465E CD8$^+$ T effectors were enriched in MPECs.

The T-box transcription factors T-bet and eomesodermin (Eomes) regulate the differentiation of CD8$^+$ T cells into effector and memory cells (4). While T-bet expression is required for the generation of KLRG1^{hi} cells (1), Eomes promotes the generation and persistence of T_{CM} (26). Examination of the expression of T-bet and Eomes revealed that PDK1-K465E OT-I effectors express similar levels of T-bet but higher levels of Eomes when

compared to PDK1-WT, suggesting a superior potential of PDK1-K465E effectors to give rise to T_{CM} (Fig. 5G and H).

The role of Akt signaling in the generation of memory responses after infection with *Listeria monocytogenes*. To assess the impact of reduced Akt activity on $CD8^+$ T cell persistence following infection, we first monitored the frequency of adoptively transferred PDK1-WT and PDK1-K465E OT-I in blood. In contrast to what we had observed following protein vaccination, the frequency of total memory PDK1-K465E OT-I cells generated by infection was similar to that of PDK1-WT OT-I cells (Fig. 6A). However, when expression of KLRG1 was taken into account, we noticed a striking reduction in the generation and persistence of $KLRG1^{hi}$ effector and memory $CD8^+$ T cells in blood, whereas the accumulation of $KLRG1^{lo}$ cells was minimally affected by the diminished Akt activity (Fig. 6B). Assessment of the PDK1-WT:PDK1-K465E memory cell ratios in different organs revealed similar numbers of PDK1-WT and PDK1-K465E cells in the spleen, preferential localization of PDK1-K465E OT-I cells in the LNs and decreased accumulation of PDK1-K465E cells in the liver and lungs (Fig. S6A). Furthermore, using CXCR3 and CD43 as markers that denote functionally distinct memory cell subsets, we found marked differences in the composition of PDK1-K465E and PDK1-WT OT-I memory cells. A significant reduction in the proportion of $CXCR3^{lo}CD43^{lo}$ cells was noted in the PDK1-K465E memory pool, accompanied by a reciprocal increase in the proportion of the $CXCR3^{hi}$ cells, in particular the $CXCR3^{hi}CD43^{lo}$ subset (Fig. 6C). This resulted in a significant decrease in the absolute numbers of PDK1-K465E $CXCR3^{lo}CD43^{lo}$ effector-like memory cells in the spleen, liver and lungs and an increase in the numbers of PDK1-K465E $CXCR3^{hi}CD43^{lo}$ cells, and to a lesser extent of PDK1-K465E $CXCR3^{hi}CD43^{hi}$ cells in spleen and LNs (Fig. 6D). Accordingly, lower numbers of PDK1-K465E cells expressing KLRG1, which is predominantly expressed on $CXCR3^{lo}CD43^{lo}$ memory cells (Fig. S2D and (8, 9)), were

recovered from the spleen, liver and lungs (Fig. S6B). Similar to what we observed for memory cells generated by protein vaccination, CXCR3^{lo}CD43^{lo}KLRG1^{hi} memory cells recovered from the lungs and liver were largely not protected from i.v. antibody labelling, suggesting that these cells were associated with the vasculature of these organs (Fig. S7). When re-stimulated *ex vivo*, PDK1-K465E memory cells were equally capable of producing IFN-γ and TNF-α as PDK1-WT cells, but they comprised a larger proportion of IL-2-producing cells (Fig. 6E and Fig. S8A and B), consistent with the altered composition of the PDK1-K465E memory population which is skewed towards the CXCR3^{hi} subset (8). Furthermore, the remaining PDK1-K465E CXCR3^{lo}CD43^{lo} memory cells expressed substantially less granzyme B compared to PDK1-WT cells (Fig. 7A and Fig. S8C). To address if the loss of CXCR3^{lo}CD43^{lo} cells from the memory population of PDK1-K465E T cells impacts on the killing capacity of memory cells, we compared PDK1-WT and PDK1-K465E memory T cells in an *ex vivo* cytotoxicity assay. PDK1-WT cells were more efficient on a per cell basis than PDK1-K465E cells in killing OVA peptide-pulsed target cells (Fig. S8D), suggesting that PDK1-WT memory cells are potentially better in conferring protective immunity *in vivo*.

To assess the impact of the altered memory pool on protective immunity *in vivo*, we injected E.G7 tumor cells into mice that had been previously challenged with Lm-OVA. Delayed tumor growth was observed in mice harbouring either PDK1-WT or PDK1-K465E OT-I memory cells compared to naive mice (Fig. 7B). However, tumor protection provided by PDK1-WT memory cells was markedly more sustained. As a result, mice bearing PDK1-WT cells exhibited significantly increased survival relative to mice bearing PDK1-K465E cells (Fig. 7C). These results highlight the importance of optimal Akt signaling in the generation of protective memory CD8$^+$ T cells. We next assessed the frequency and phenotype of tumor-infiltrating CD8$^+$ T cells (TILs). The frequencies of PDK1-WT and

PDK1-K465E T cells among tumor-infiltrating $CD8^+$ T cells were similar (Fig. S9A). Unexpectedly, CXCR3 was downregulated on TILs compared to splenic $CD8^+$ T cells (Fig. S9B), therefore preventing its use as a marker to delineate the memory $CD8^+$ T cell subsets. However, the chemokine receptor CX_3CR1, recently shown to be expressed on effector-like memory $CD8^+$ T cells (27) and confirmed by us (Fig. S9C), was expressed on a sub-population of TILs (Fig. S9D). Importantly, we show that the frequency of CX_3CR1^+ cells was reduced among PDK1-K465E TILs compared to PDK1-WT TILs, suggesting that optimal accumulation of tumor-associated effector-like memory cells is dependent on Akt activity (Fig. S9D and E).

Discussion

In the present study we explored how PIP3-dependent activation of Akt impacts on the $CD8^+$ T cell response elicited by vaccination or infection. The overarching conclusion from the current study is that $CD8^+$ T cell expansion and acquisition of effector function during the primary response are relatively insensitive to sub-optimal Akt activity, whereas multiple aspects of protective memory cell development are highly dependent on Akt signaling.

The current study demonstrates that maximal Akt signaling is neither required for $CD8^+$ T cell expansion, nor is it necessary for generation of CTLs during the primary response. Although primary PDK1-K465E OT-I effector T cells express marginally lower levels of granzyme B compared to PDK1-WT cells, they produce similar levels of IFN-γ and TNF-α. Importantly, we show that maximal Akt activity is not required for the anti-tumor response during the primary effector phase, since PDK1-K465E OT-I effector cells provide equivalent protection against E.G7 tumors as PDK1-WT OT-I effectors. Although we cannot exclude the possibility that the residual Akt activity in PDK1-K465E T cells was sufficient for generation of primary effectors, an alternative explanation is that the primary T cell response is largely controlled by other signaling pathways. Notably, mTORC1 activity has been shown to be necessary for optimal $CD8^+$ T cell expansion and differentiation into effector cells (28). In this context, activation of mTORC1 in $CD8^+$ T cells is independent of Akt activity ((16) and Fig. S1A and B). By controlling the expression of hypoxia-inducible factor 1, mTORC1 enhances glucose metabolism and glycolysis and regulates the expression of perforin, granzymes, CD62L and CCR7 (16). Therefore, there is some redundancy in the effects of Akt and mTORC1 signaling on the regulation of cytotoxicity and tissue trafficking.

A striking finding of the current study is that Akt activity in $CD8^+$ T cells is required for cell survival during the transition from the effector to the memory cell stage after protein vaccination. Reduced Akt activity had profound effects on the overall number of vaccine-generated memory cells such that after re-challenge the magnitude of the secondary response was significantly diminished. The pro-survival role of Akt in $CD8^+$ T cells during the contraction phase is supported by our finding that the levels of the pro-apoptotic Bcl2 family protein Bim are elevated in PDK1-K465E effector T cells after protein vaccination. Bim is known to promote the contraction phase of $CD8^+$ effector T cells (23) and its expression in T cell lines is upregulated by Foxo3 (29). In this respect, recent studies have shown that deletion of Foxo3 in T cells results in an increase in T cell survival either during the primary response or the contraction phase concomitant with reduced expression of Bim (30-32). Foxo3 is phosphorylated by Akt, a posttranslational modification that results in Foxo3 nuclear exclusion and translocation to the cytosol (29). Hence, the finding that PDK1-K465E effectors express elevated levels of Bim is consistent with the notion that reduced Akt signaling results in Foxo3-dependent upregulation of Bim.

By extending our analysis to an infection model, we found that Akt signaling is primarily required for the differentiation of $CD8^+$ T cells into $CXCR3^{lo}CD43^{lo}KLRG1^{hi}$ effector-like memory $CD8^+$ T cells. The reduction in the number of effector-like memory PDK1-K465E OT-I cells followed a decline in $KLRG1^{hi}$ effectors, suggesting that the lack of Akt signaling had an early impact on the generation of this population. In addition, the frequency of IL-2-secreting cells among effector and memory cells mirrored the phenotypic changes, consistent with previous studies demonstrating that $KLRGl^{hi}$ effectors and effector-like memory cells produce less IL-2 compared to $KLRG1^{lo}$ effectors and T_{CM} (1, 8, 24). Since the transcription factors T-bet and Eomes have crucial roles in the generation of $KLRG1^{hi}$ effectors and T_{CM}, respectively (4), we assessed whether reduced Akt signaling

impacts on their expression. T-bet expression within effectors was not altered by the reduction in Akt signaling, suggesting that Akt promotes the generation of KLRG1^{hi} effectors and effector like-memory T cells by an independent mechanism. In contrast, expression of Eomes among PDK1-K465E OT-I effectors was increased when compared to its levels in PDK1-WT OT-I effectors. Previous work has shown that CD8$^+$ effector T cells that lack Eomes generate fewer T_{CM} (26). However, Eomes does not appear to play a role in the generation of MPECs, since both MPECs and SLECs express similar amounts of Eomes and deficiency of Eomes does not alter the SLEC/MPEC ratio (26). Thus, the higher expression of Eomes among PDK1-K465E OT-I effectors when compared to PDK1-WT OT-I cells does not simply reflect the larger frequency of MPECs, but instead indicates that Akt signaling actively suppresses Eomes expression. This suggests that Akt signaling normally limits T_{CM} generation and skews differentiation towards effector-like memory T cells at least in part through downregulation of Eomes. Eomes expression is dependent on the transcription factor Foxo1, which is a known target for Akt-mediated phosphorylation and inactivation (20, 33). Thus, the data presented herein place Akt at the apex of the CD8$^+$ T cell differentiation program that controls effector-like memory cells and T_{CM}.

Generation of protective long-lasting CD8$^+$ T cell-dependent immunity is an important goal for anti-cancer vaccines. Here we show that Akt signaling is required for long-term protective anti-tumor immunity in two different settings. In the protein vaccination approach, the diminished anti-tumor protection was primarily the result of the vastly reduced numbers of memory PDK1-K465E OT-I cells. Reduction in secondary effector differentiation, exemplified by lower granzyme B expression upon peptide boosting, may have also contributed to the lack of anti-tumor activity of memory PDK1-K465E T cells. In the second approach, T cells were primed with Lm-OVA. This setting generated similar numbers of total PDK1-K465E and PDK1-WT OT-I memory cells, but the PDK1-K465E

memory population was largely devoid of CXCR3^{lo}CD43^{lo} effector-like memory cells with the remaining CXCR3^{lo}CD43^{lo} cells expressing diminished amounts of granzyme B. Consequently when we compared the cytotoxicity of PDK1-K465E and PDK1-WT OT-I memory cells we found that on a per cell basis PDK1-K465E T cells were less efficient in killing than PDK1-WT T cells. In addition assessment of their anti-tumor activity *in vivo* without further boosting showed that memory PDK1-K465E T cells were less effective in providing long-term protection than PDK1-WT T cells. These findings ascribe an important function for Akt in tumor immune surveillance by memory CD8$^+$ T cells. Recently, Crompton et al (12) showed that pharmacological inhibition of Akt during *in vitro* expansion of tumor reactive T cells results in enhanced persistence and anti-tumor activity upon adoptive transfer and boosting. T cell expansion protocols for adoptive T cell therapy typically use anti-CD3 antibody and high dose IL-2, conditions that promote sustained Akt signaling and terminal differentiation of effector CD8$^+$ T cells at the expense of T_{CM} generation (14, 34). Under these conditions inhibition of Akt is expected to enhance the efficacy of adoptive T cell therapy by reducing the generation of terminally differentiated effector cells (12). However, our findings suggest that the physiological role of Akt in immune responses is to promote the generation of effector-like memory cells which along with other memory subsets ensure maximal protection of the host against antigen re-encounter.

The data presented in the current study also demonstrate that the type of immune challenge dictates which facet of memory cell development is affected by Akt signaling. Whereas differentiation into effector-like memory T cells was similarly affected in the protein vaccination and infection models, its pro-survival effects during the contraction phase were confined to responses elicited by protein vaccination. Interestingly, Bim was similarly expressed in PDK1-K465E OT-I and PDK1-WT OT-I effectors in the infection model (Fig.

S10), which contrasts with the results obtained following protein vaccination (Fig. 4C). This may explain why primary PDK1-K465E OT-I effectors underwent a more pronounced contraction, compared to PDK1-WT OT-I effectors, after protein vaccination but not following infection. Different mechanisms of Foxo3 regulation that subsequently influence Bim expression could be operating depending on the type of immune challenge. Thus, besides Akt, Erk and IKK have been shown to inhibit Foxo3 activity and various pathways are known to counter Foxo3 inhibition (35). In addition, Bim is regulated by Foxo3-independent transcriptional, post-transcriptional and post-translational mechanisms (36), which could differ depending on the strength/duration of TCR signaling, costimulation and inflammation.

Finally, the effects of Akt signaling reported herein are similar to those ascribed to IL-2 in the generation of memory cell subsets (2, 3), suggesting that Akt signaling is the primary mechanism responsible for these effects. In summary, the present study demonstrates a previously unappreciated role for Akt in the generation of protective memory $CD8^+$ T cell responses, notably against tumor recurrence. Optimizing Akt activity should therefore maximize the therapeutic effect of anti-cancer vaccines.

Materials and Methods

Mice and *in vivo* experiments. All procedures were conducted in accordance with UK Home Office guidelines and approved by the University of Southampton's ethical committee. C57BL/6 mice were obtained from Charles River. OT-I transgenic mice carrying the K465E knock-in mutation in the PH domain of PDK1 (*Pdpk1*^{K465E}) have been described previously (13, 14). Unless otherwise specified, 10^4 CD45.1 or CD45.1/CD45.2 OT-I cells isolated from spleen were transferred i.v. into CD45.2 C57BL/6 recipient mice. For co-transfer experiments, $5x10^3$ CD45.1 PDK1-WT OT-I were mixed with $5x10^3$ CD45.1/CD45.2 PDK1-K465E OT-I and transferred i.v. to CD45.2 C57BL/6 mice. One day later, mice were challenged i.p. with OVA (5 mg, Sigma) plus anti-CD40 mAb (100 µg, clone 3/23, (37)) and 10 µg LPS (Sigma) or OVA plus anti-4-1BB mAb (200 µg, clone Lob12.3, (38)) and LPS or OVA plus polyI:C (50 µg, Sigma). Alternatively, mice were infected with 10^6 CFU of ΔActA-*Listeria monocytogenes*-OVA i.v. (DMX, Philadelphia). In some experiments, mice were re-challenged with 30 nmols $OVA_{257-264}$ peptide i.v. alone (in the case of OVA/anti-CD40/LPS priming) or mixed with 100 µg anti-CD40 mAb (when using OVA/anti-41BB/LPS and OVA/polyI:C for priming). Where indicated mice were injected s.c. with OVA-expressing E.G7 tumor cells (ATCC). Tumor growth was monitored and mice were sacrificed when the humane endpoint was reached (15 mm mean tumor diameter when taking the two greatest perpendicular measurements).

Flow cytometry. Antibodies and methods are listed in the supporting information. PE-labelled H-2K^b/SIINFEKL tetramer was prepared in-house. Samples were analyzed with a FACS Canto II and DIVA Software (BD Biosciences) or FCS Express (De Novo Software).

Lymphocyte isolation from non-lymphoid tissues. Colon lamina propria lymphocytes were isolated as described previously (39), except that collagenase VIII was used for enzymatic digestion (0.2 mg/mL, Sigma). PBS-washed livers were homogenized through a 100 μm-cell strainer in PBS containing 0.5% FCS and 2 mM EDTA. After centrifugation, cell pellet was resuspended in 40% Percoll solution (GE Healthcare) and layered on 70% Percoll solution. Cells recovered at the interface were washed twice in PBS. The same protocol was applied to lungs, except they were first cut into small pieces.

Western Blotting. Detailed protocols of cell preparation are given in the supporting information. Cell lysates were prepared as previously described (16), proteins were separated using NuPage Bis-Tris gels (Life Technologies) and transferred to PVDF membranes (Immobilon-P, Millipore). Blots were probed with antibodies listed in the supporting information. Densitometry analysis was performed using ImageJ software.

Statistical analysis. Where indicated p values (*$p \leq 0.05$, **$p \leq 0.01$, ***$p \leq 0.001$) were determined by a two-tailed unpaired Student's t test using Prism (GraphPad software), except for survival curves where a Mantel-Cox log-rank test was used.

Additional materials and methods are available in SI Material and Methods.

Acknowledgements

We thank D. Cantrell and D. Alessi (University of Dundee) for providing the *Pdpk1*^{K465E} knockin mice and for helpful discussions and review of data. We thank members of the Biomedical Research Facility (University of Southampton) for excellent support in management of the mouse colonies, L. Douglas and P. Duriez (CRUK protein production facility, University of Southampton) for the PE-labelled H-2K^{b}/SIINFEKL tetramer. The work was funded by CRUK project grants 8444 and 13211.

Footnotes

[1]To whom correspondence should be addressed. Email:aymen@soton.ac.uk

Author contributions: A.R., J.E.W., S.L.B. H.J.L. and S.M.T. performed the experiments and analyzed the data; A.Al-S designed and supervised the research and A.R., S.L.B. and A.Al-S. wrote the manuscript.

References

1. Joshi NS*, et al.* (2007) Inflammation directs memory precursor and short-lived effector CD8(+) T cell fates via the graded expression of T-bet transcription factor. *Immunity* 27(2):281-295.
2. Kalia V*, et al.* (2010) Prolonged interleukin-2Ralpha expression on virus-specific CD8+ T cells favors terminal-effector differentiation *in vivo*. *Immunity* 32(1):91-103.
3. Mitchell DM, Ravkov EV, & Williams MA (2010) Distinct roles for IL-2 and IL-15 in the differentiation and survival of CD8+ effector and memory T cells. *Journal of immunology* 184(12):6719-6730.
4. Kaech SM & Cui W (2012) Transcriptional control of effector and memory CD8+ T cell differentiation. *Nature reviews. Immunology* 12(11):749-761.
5. Sallusto F, Lenig D, Forster R, Lipp M, & Lanzavecchia A (1999) Two subsets of memory T lymphocytes with distinct homing potentials and effector functions. *Nature* 401(6754):708-712.
6. Wherry EJ*, et al.* (2003) Lineage relationship and protective immunity of memory CD8 T cell subsets. *Nature immunology* 4(3):225-234.
7. Wolint P, Betts MR, Koup RA, & Oxenius A (2004) Immediate cytotoxicity but not degranulation distinguishes effector and memory subsets of CD8+ T cells. *The Journal of experimental medicine* 199(7):925-936.
8. Hikono H*, et al.* (2007) Activation phenotype, rather than central- or effector-memory phenotype, predicts the recall efficacy of memory CD8+ T cells. *The Journal of experimental medicine* 204(7):1625-1636.
9. Olson JA, McDonald-Hyman C, Jameson SC, & Hamilton SE (2013) Effector-like CD8(+) T cells in the memory population mediate potent protective immunity. *Immunity* 38(6):1250-1260.
10. Cantrell D (2015) Signaling in lymphocyte activation. *Cold Spring Harbor perspectives in biology* 7(6).
11. Macintyre AN*, et al.* (2011) Protein kinase B controls transcriptional programs that direct cytotoxic T cell fate but is dispensable for T cell metabolism. *Immunity* 34(2):224-236.
12. Crompton JG*, et al.* (2015) Akt inhibition enhances expansion of potent tumor-specific lymphocytes with memory cell characteristics. *Cancer research* 75(2):296-305.
13. Bayascas JR*, et al.* (2008) Mutation of the PDK1 PH domain inhibits protein kinase B/Akt, leading to small size and insulin resistance. *Molecular and cellular biology* 28(10):3258-3272.
14. Waugh C, Sinclair L, Finlay D, Bayascas JR, & Cantrell D (2009) Phosphoinositide (3,4,5)-triphosphate binding to phosphoinositide-dependent kinase 1 regulates a protein kinase B/Akt signaling threshold that dictates T-cell migration, not proliferation. *Molecular and cellular biology* 29(21):5952-5962.
15. Mao C*, et al.* (2007) Unequal contribution of Akt isoforms in the double-negative to double-positive thymocyte transition. *Journal of immunology* 178(9):5443-5453.
16. Finlay DK*, et al.* (2012) PDK1 regulation of mTOR and hypoxia-inducible factor 1 integrate metabolism and migration of CD8+ T cells. *The Journal of experimental medicine* 209(13):2441-2453.
17. Lefrancois L, Altman JD, Williams K, & Olson S (2000) Soluble antigen and CD40 triggering are sufficient to induce primary and memory cytotoxic T cells. *Journal of immunology* 164(2):725-732.
18. Ahonen CL*, et al.* (2004) Combined TLR and CD40 triggering induces potent CD8+ T cell expansion with variable dependence on type I IFN. *The Journal of experimental medicine* 199(6):775-784.
19. Anderson KG*, et al.* (2014) Intravascular staining for discrimination of vascular and tissue leukocytes. *Nature protocols* 9(1):209-222.

20. Hess Michelini R, Doedens AL, Goldrath AW, & Hedrick SM (2013) Differentiation of CD8 memory T cells depends on Foxo1. *The Journal of experimental medicine* 210(6):1189-1200.
21. Kim MV, Ouyang W, Liao W, Zhang MQ, & Li MO (2013) The transcription factor Foxo1 controls central-memory CD8+ T cell responses to infection. *Immunity* 39(2):286-297.
22. Kerdiles YM*, et al.* (2009) Foxo1 links homing and survival of naive T cells by regulating L-selectin, CCR7 and interleukin 7 receptor. *Nature immunology* 10(2):176-184.
23. Hildeman DA*, et al.* (2002) Activated T cell death *in vivo* mediated by proapoptotic bcl-2 family member bim. *Immunity* 16(6):759-767.
24. Sarkar S*, et al.* (2008) Functional and genomic profiling of effector CD8 T cell subsets with distinct memory fates. *The Journal of experimental medicine* 205(3):625-640.
25. Cui W, Joshi NS, Jiang A, & Kaech SM (2009) Effects of Signal 3 during CD8 T cell priming: Bystander production of IL-12 enhances effector T cell expansion but promotes terminal differentiation. *Vaccine* 27(15):2177-2187.
26. Banerjee A*, et al.* (2010) Cutting edge: The transcription factor eomesodermin enables CD8+ T cells to compete for the memory cell niche. *Journal of immunology* 185(9):4988-4992.
27. Bottcher JP*, et al.* (2015) Functional classification of memory CD8(+) T cells by CX3CR1 expression. *Nature communications* 6:8306.
28. Pollizzi KN*, et al.* (2015) mTORC1 and mTORC2 selectively regulate CD8(+) T cell differentiation. *The Journal of clinical investigation* 125(5):2090-2108.
29. Stahl M*, et al.* (2002) The forkhead transcription factor FoxO regulates transcription of p27Kip1 and Bim in response to IL-2. *Journal of immunology* 168(10):5024-5031.
30. Sullivan JA, Kim EH, Plisch EH, Peng SL, & Suresh M (2012) FOXO3 regulates CD8 T cell memory by T cell-intrinsic mechanisms. *PLoS pathogens* 8(2):e1002533.
31. Tzelepis F*, et al.* (2013) Intrinsic role of FoxO3a in the development of CD8+ T cell memory. *Journal of immunology* 190(3):1066-1075.
32. Togher S, Larange A, Schoenberger SP, & Feau S (2015) FoxO3 is a negative regulator of primary CD8+ T-cell expansion but not of memory formation. *Immunology and cell biology* 93(2):120-125.
33. Rao RR, Li Q, Gubbels Bupp MR, & Shrikant PA (2012) Transcription factor Foxo1 represses T-bet-mediated effector functions and promotes memory CD8(+) T cell differentiation. *Immunity* 36(3):374-387.
34. Pipkin ME*, et al.* (2010) Interleukin-2 and inflammation induce distinct transcriptional programs that promote the differentiation of effector cytolytic T cells. *Immunity* 32(1):79-90.
35. Hedrick SM, Hess Michelini R, Doedens AL, Goldrath AW, & Stone EL (2012) FOXO transcription factors throughout T cell biology. *Nature reviews. Immunology* 12(9):649-661.
36. Sionov RV, Vlahopoulos SA, & Granot Z (2015) Regulation of Bim in Health and Disease. *Oncotarget* 6(27):23058-23134.
37. Taraban VY, Rowley TF, & Al-Shamkhani A (2004) Cutting edge: a critical role for CD70 in CD8 T cell priming by CD40-licensed APCs. *Journal of immunology* 173(11):6542-6546.
38. Taraban VY*, et al.* (2002) Expression and costimulatory effects of the TNF receptor superfamily members CD134 (OX40) and CD137 (4-1BB), and their role in the generation of anti-tumor immune responses. *European journal of immunology* 32(12):3617-3627.
39. Uhlig HH*, et al.* (2006) Characterization of Foxp3+CD4+CD25+ and IL-10-secreting CD4+CD25+ T cells during cure of colitis. *Journal of immunology* 177(9):5852-5860.

Figures legends

Fig. 1. Reduced Akt signaling does not impede the generation of primary effectors. Following adoptive transfer of CD45.1 PDK1-WT or PDK1-K465E OT-I, congenic recipient mice were vaccinated with OVA/anti-CD40 mAb/LPS. Spleens, inguinal LNs and blood samples were harvested 6 days later. *(A)* Numbers of CD45.1 Tetramer$^+$ PDK1-WT and PDK1-K465E cells in spleen, LNs and blood. *(B)* Frequency of splenic CD45.1 OT-I cells expressing granzyme B. Right panel shows representative histogram overlays of the expression of granzyme B in PDK1-WT (shaded histograms) and PDK1-K465E OT-I (black line). Dotted lines show the corresponding isotypes. *(C)* Frequency of splenic CD45.1 OT-I cells producing IFN-γ, TNF-α or IL-2, following *ex vivo* re-stimulation with 10 pM or 1 nM of $OVA_{257-264}$. *(A-C)* Data show the mean ± SEM of two combined experiments, with n=4 mice/group. *(D)* 4 days before adoptive transfer and vaccination with OVA/anti-CD40/LPS, mice received $2.5x10^5$ E.G7 tumor cells s.c.. Left panel shows the mean tumor diameter ± SEM of one experiment representative of 2 with n=5-6 mice/group. Right panel shows the mean tumor diameter ± SEM of 2 combined experiments on day 18 after tumor injection, with each symbol representing an individual mouse. **p≤ 0.01, ***p≤ 0.001.

Fig. 2. Akt signaling is required for the generation of memory cells following protein vaccination. Mice received either a single transfer *(A, C, D)* or a 1:1 co-transfer *(B)* of PDK1-WT and PDK1-K465E OT-I cells and were then vaccinated with OVA/anti-CD40/LPS. *(A)* Frequency of CD45.1 Tetramer$^+$ OT-I cells in blood. *(B)* Proportion of PDK1-WT and PDK1-K465E OT-I cells among CD45.1 donor cells following co-transfer. *(C)* Absolute numbers of CD45.1 Tetramer$^+$ OT-I cells in various organs (LP; lamina propria) 12 weeks post-vaccination. *(D)* Pie charts depicting the frequency of $CXCR3^{hi}CD43^{lo}$, $CXCR3^{hi}CD43^{hi}$ and $CXCR3^{lo}CD43^{lo}$ cells among donor OT-I cells 6-7 weeks post-priming. Statistical differences between PDK1-WT and PDK1-K465E OT-I are given for each subset.

Data show the mean ± SEM of *(A)* one experiment representative of 4 with n=5-10 mice/group, *(B)* one experiment with n=5 mice, *(C)* one representative experiment with n=5 mice/group, and *(D)* data are combined from 2 independent experiments with n=3 mice/group. *p≤ 0.05, **p≤ 0.01, ***p≤ 0.001, ns; not significant.

Fig. 3. Loss of PDK1-K465E OT-I memory cells following vaccination results in a diminished recall response. Adoptive cell transfer and vaccination with OVA/anti-CD40/LPS were performed as in Fig. 1. *(A)* Frequency of CD45.1 Tetramer$^+$ OT-I cells in blood following priming with OVA/anti-CD40/LPS and re-challenge (indicated by the arrow) with $OVA_{257-264}$. *(B)* Frequency of CD45.1 OT-I cells expressing granzyme B cells in blood on day 4 and day 7 after re-challenge, with each data point representing an individual mouse. *(C)* Mice received $5x10^5$ E.G7 tumour cells s.c. on day 3 post-re-challenge. Left panel shows the mean tumor diameter ± SEM. Right panel shows the mean tumor diameter ± SEM on day 19 after tumor injection, with each symbol representing an individual mouse. Data show the mean ± SEM of *(A)* one experiment representative of 3 with n=5-10 mice/group, *(B)* one experiment with n=3-8 mice/group, *(C)* one experiment with n=10 mice/group. *p≤ 0.05, **p≤ 0.01.

Fig. 4. Bim expression is increased in PDK1-K465E OT-I effectors. Adoptive cell transfer and vaccination with OVA/anti-CD40/LPS were performed as in Fig. 1. *(A)* Representative dot plots of CD127 and KLRG1 expression and *(B)* Frequency of $CD127^{hi}KLRG1^{lo}$ and $CD127^{lo}KLRG1^{hi}$ cells among PDK1-WT and PDK1-K465E OT-I cells in spleen on day 6 post-priming. *(C)* On day 7 post-vaccination, Bim and actin expression levels in purified splenic PDK1-WT and PDK1-K465E OT-I cells were analyzed by Western Blotting and densitometry. Bar graphs represent the ratio of Bim to actin expressed as % of PDK1-WT values. Data show the mean ± SEM of *(B)* 2 combined experiments, with n=4 mice/group and *(C)* 3 combined experiments with n=2 mice/group. **p≤ 0.01.

Fig. 5. Akt signaling regulates the differentiation of KLRG1^{hi} effectors following *Listeria monocytogenes* infection. Mice received either a single transfer (filled symbols) or a co-transfer (open symbols) of PDK1-WT and PDK1-K465E OT-I cells and were challenged one day later with ΔActA-Lm-OVA. Spleen, inguinal LNs and blood samples were harvested 6 days later and the frequency and phenotype of OT-I cells were analyzed by flow cytometry. *(A)* Frequency of OT-I cells among CD8^{+} T cells and *(B)* PDK1-WT:PDK1-K465E OT-I cell ratio in the different tissues. *(C)* Frequency of CD62L^{hi} cells among OT-I cells in spleen. Frequency and numbers of *(D)* KLRG1^{hi} cells and *(E)* CD127^{hi} cells in spleen. *(F)* Frequency of splenic PDK1-WT and PDK1-K465E OT-I producing IL-2 following *ex vivo* re-stimulation with 10 pM or 1 nM of $OVA_{257-264}$. *(G)* Representative histogram overlays of Eomes and T-bet expression in PDK1-WT (shaded histogram) and PDK1-K465E OT-I cells (black line). Dotted lines show the corresponding isotypes. *(H)* Frequency of Eomes^{hi} and T-bet^{+} cells among OT-I cells in spleen. Data are *(A,B)* from one experiment representative of 2 with n=3-5 mice/experiment, *(C-F, H)* combined from 2 independent experiments, with each symbol representing an individual mouse. Mean ± SEM is shown. *p≤ 0.05, ***p≤ 0.001.

Fig. 6. Akt signaling in CD8^{+} T cells regulates the composition of memory cells after *Listeria monocytogenes* infection. Co-transfer of PDK1-WT and PDK1-K465E OT-I cells and infection with ΔActA-Lm-OVA were performed as in Fig. 5. *(A,B)* Blood samples were analyzed at the indicated time points and *(C-E)* spleen, inguinal LNs, liver and lungs were harvested 6-9 weeks following infection. *(A)* Frequency of OT-I cells among CD8^{+} T cells in blood. *(B)* Numbers of KLRG1^{hi} (left panel) or KLRG1^{lo} (right panel) OT-I cells per mL of blood. *(C)* Pie charts depicting the frequency of CXCR3^{hi}CD43^{lo}, CXCR3^{hi}CD43^{hi} and CXCR3^{lo}CD43^{lo} cells among OT-I cells. Statistical differences between PDK1-WT and PDK1-K465E OT-I are given for each subset. *(D)* Numbers of CXCR3^{hi}CD43^{lo}, CXCR3^{hi}CD43^{hi} and CXCR3^{lo} CD43^{lo} memory cells. *(E)* Frequency of PDK1-WT and

PDK1-K465E OT-I cells producing IFN-γ, TNF-α or IL-2 in spleen, following *ex vivo* re-stimulation with 1 nM of $OVA_{257-264}$. Data show *(A, B)* the mean ± SEM of one experiment representative of 3, with n=5-10 mice/experiment and *(E)* the mean of 2 combined experiments with n=4-6 mice/experiment, with each symbol representing an individual mouse. *(C, D)* Spleen data are representative of 3 independent experiments with n=4-6 mice/experiment; LN, liver and lungs data are representative of 2 experiments with n=4 mice/experiment. Data show the mean ± SEM and each symbol represents an individual mouse. *p≤ 0.05, **p≤ 0.01, ***p≤ 0.001, ns; not significant.

Fig. 7. PDK1-K465E memory cells formed after Listeria-OVA infection fail to provide long-term protection against E.G7 tumors. After adoptive transfer and infection with ΔActA-Lm-OVA, mice were challenged on day 62, without further boosting, with $5x10^5$ E.G7 tumor cells (s.c.). Control mice received tumor cells only. *(A)* Left panels, dot plots show a representative example of CXCR3 and CD43 expression on PDK1-WT and PDK1-K465E memory cells in spleen prior to tumor challenge. Right panels, histograms show the expression of granzyme B in $CXCR3^{lo}CD43^{lo}$ memory cells. *(B)* Mean tumor diameter ± SEM. *(C)* Kaplan-Meier analysis of survival of naive mice and mice bearing PDK1-WT or PDK1-K465E memory cells. Data are representative of 2 independent experiments with n = 7-8 mice/group. *p≤ 0.05, ***p≤ 0.001.

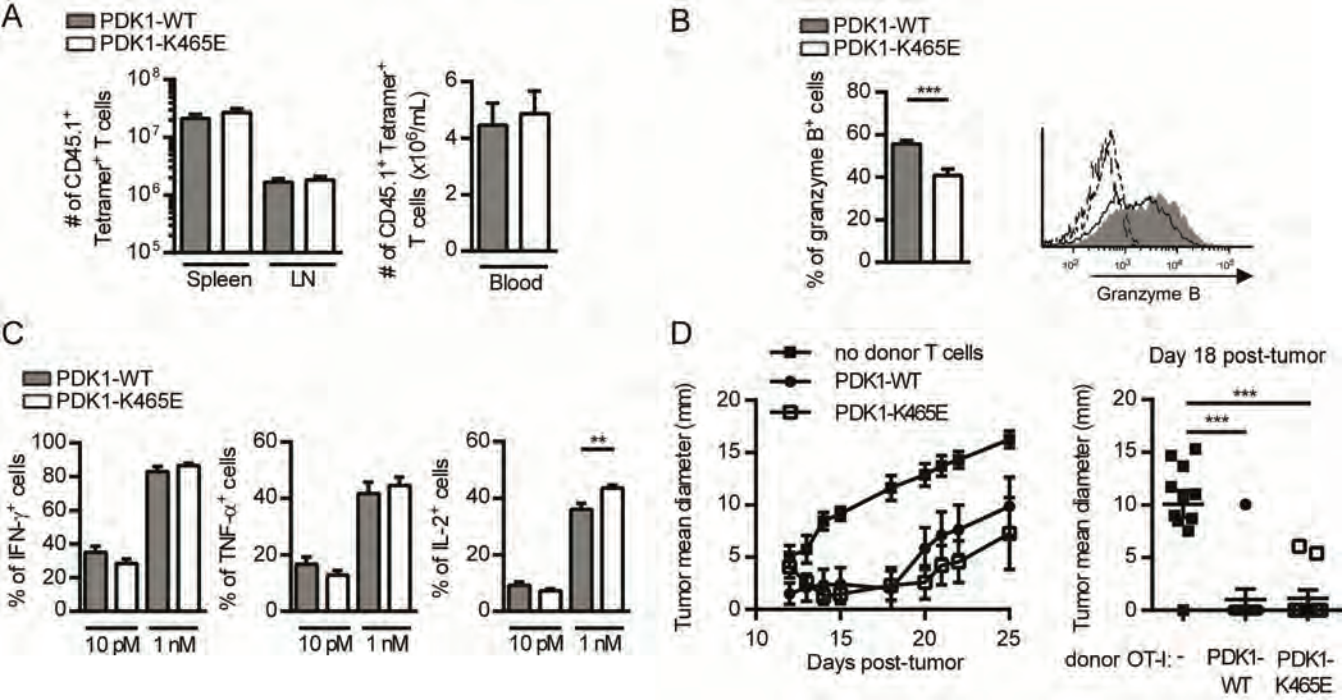
A
PDK1-WT
PDK1-K465E
# of CD45.1+ Tetramer+ T cells
Spleen
LN
# of CD45.1+ Tetramer+ T cells (x10^6/mL)
Blood
B
PDK1-WT
PDK1-K465E
% of granzyme B+ cells
***
Granzyme B
C
PDK1-WT
PDK1-K465E
% of IFN-γ+ cells
% of TNF-α+ cells
% of IL-2+ cells
**
10 pM
1 nM
D
no donor T cells
PDK1-WT
PDK1-K465E
Tumor mean diameter (mm)
Days post-tumor
Day 18 post-tumor
***
donor OT-I: -
PDK1-WT
PDK1-K465E

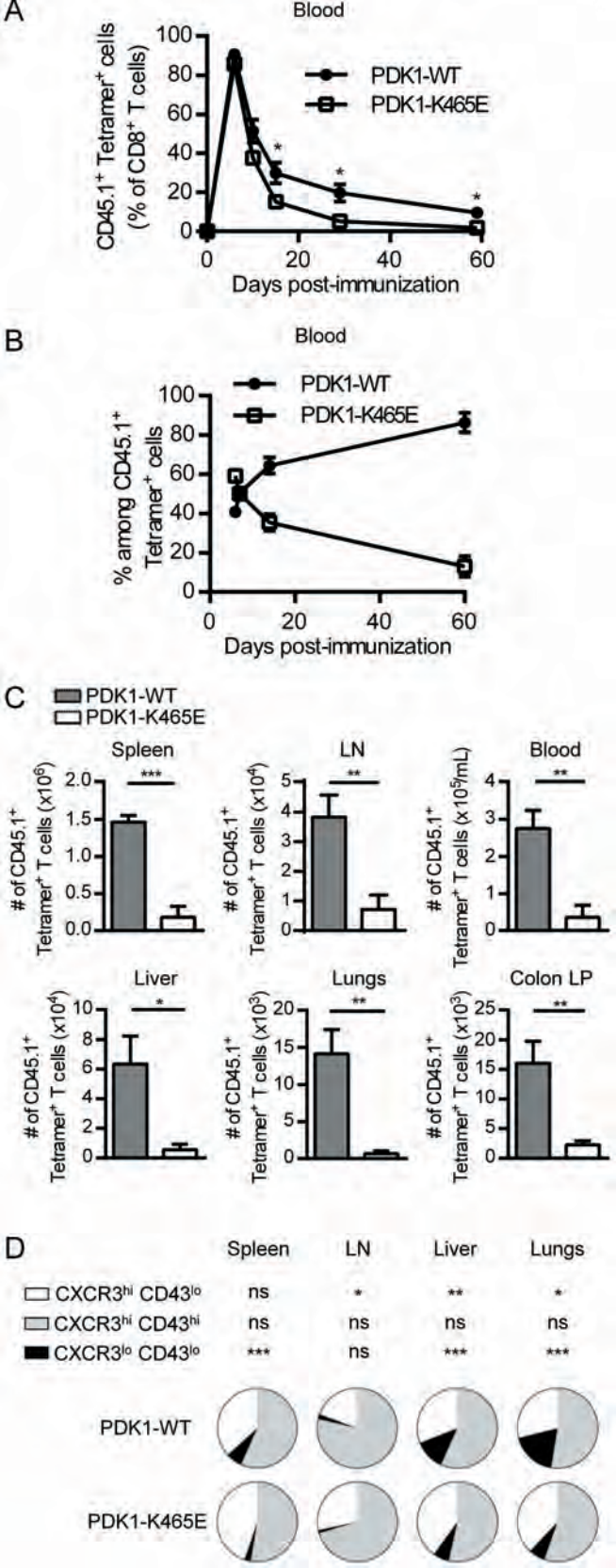
A
Blood
CD45.1+ Tetramer+ cells (% of CD8+ T cells)
PDK1-WT
PDK1-K465E
Days post-immunization
B
Blood
% among CD45.1+ Tetramer+ cells
PDK1-WT
PDK1-K465E
Days post-immunization
C
PDK1-WT
PDK1-K465E
Spleen
LN
Blood
Liver
Lungs
Colon LP
# of CD45.1+ Tetramer+ T cells
D
Spleen
LN
Liver
Lungs
CXCR3hi CD43lo
CXCR3hi CD43hi
CXCR3lo CD43lo
PDK1-WT
PDK1-K465E

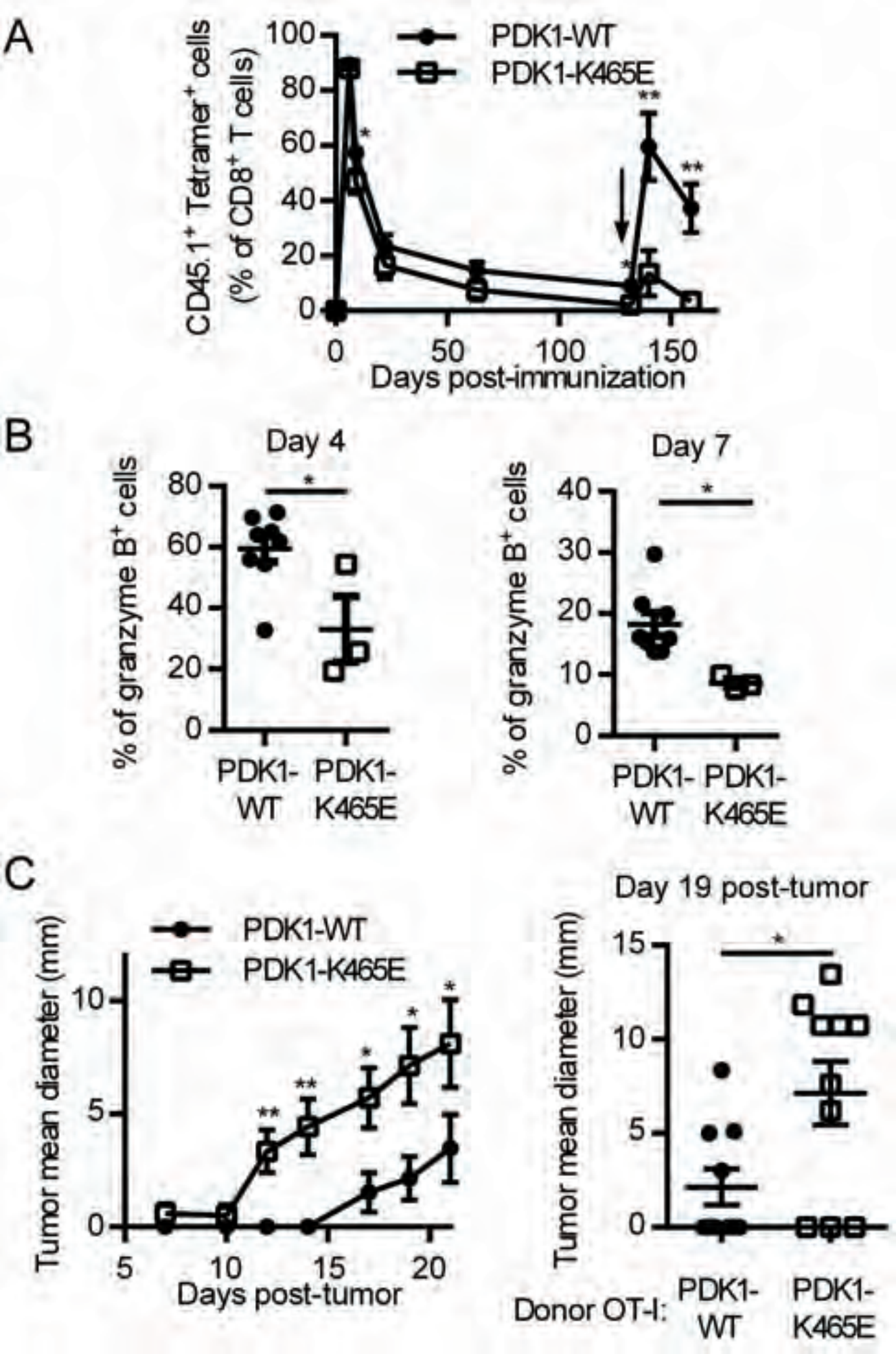
A
CD45.1+ Tetramer+ cells (% of CD8+ T cells)
PDK1-WT
PDK1-K465E
Days post-immunization
B
Day 4
Day 7
% of granzyme B+ cells
PDK1-WT
PDK1-K465E
C
Tumor mean diameter (mm)
Days post-tumor
Day 19 post-tumor
Donor OT-I:

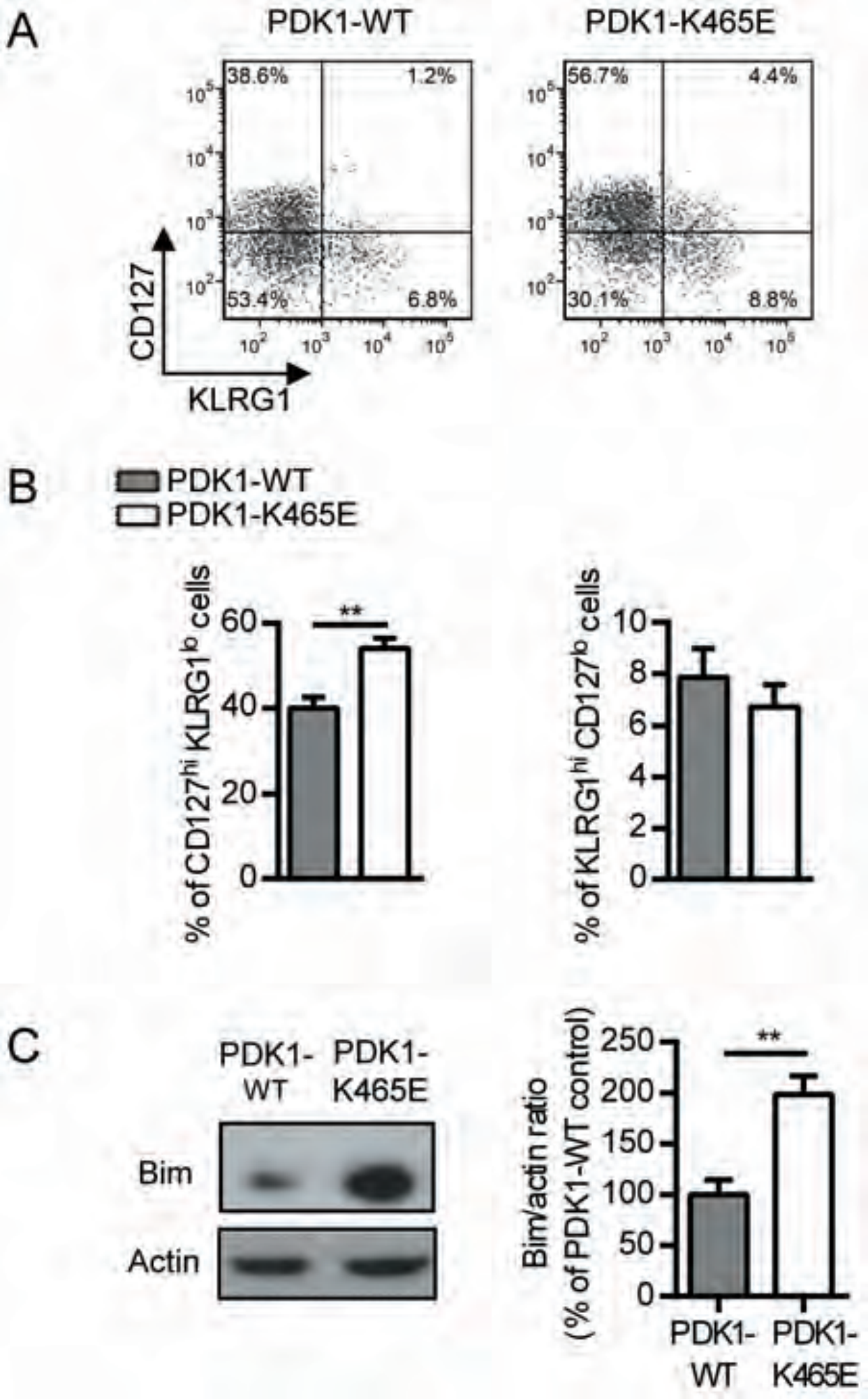
A
PDK1-WT
PDK1-K465E
38.6%
1.2%
53.4%
6.8%
56.7%
4.4%
30.1%
8.8%
CD127
KLRG1
B
PDK1-WT
PDK1-K465E
% of CD127hi KLRG1lo cells
% of KLRG1hi CD127lo cells
**
C
PDK1-WT
PDK1-K465E
Bim
Actin
Bim/actin ratio (% of PDK1-WT control)
**
PDK1-WT
PDK1-K465E

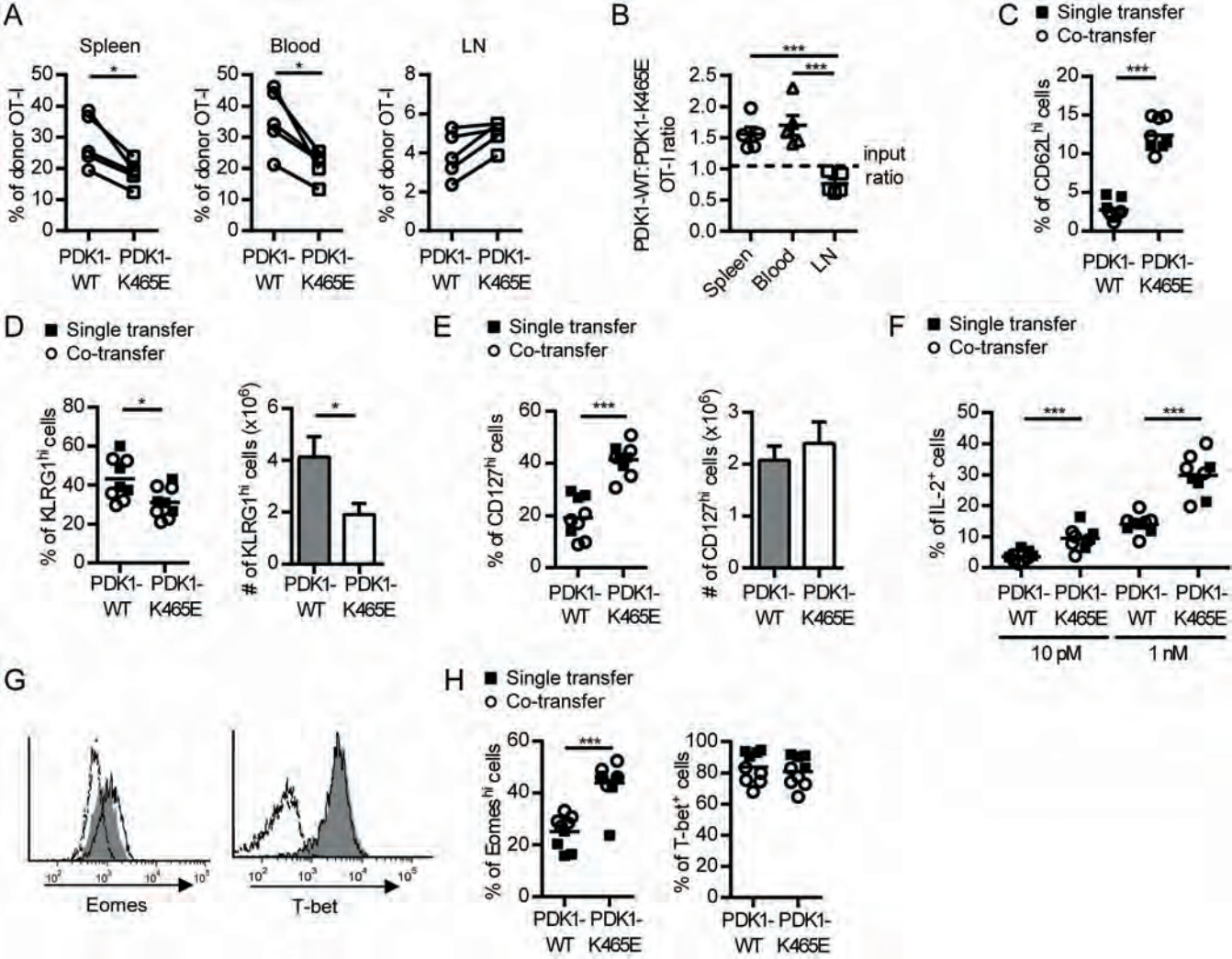
A
Spleen
Blood
LN
% of donor OT-I
PDK1-WT
PDK1-K465E
B
PDK1-WT:PDK1-K465E OT-I ratio
input ratio
Spleen
Blood
LN
C
Single transfer
Co-transfer
% of CD62L^hi cells
D
% of KLRG1^hi cells
# of KLRG1^hi cells (x10^6)
E
% of CD127^hi cells
# of CD127^hi cells (x10^6)
F
% of IL-2^+ cells
10 pM
1 nM
G
Eomes
T-bet
H
% of Eomes^hi cells
% of T-bet^+ cells

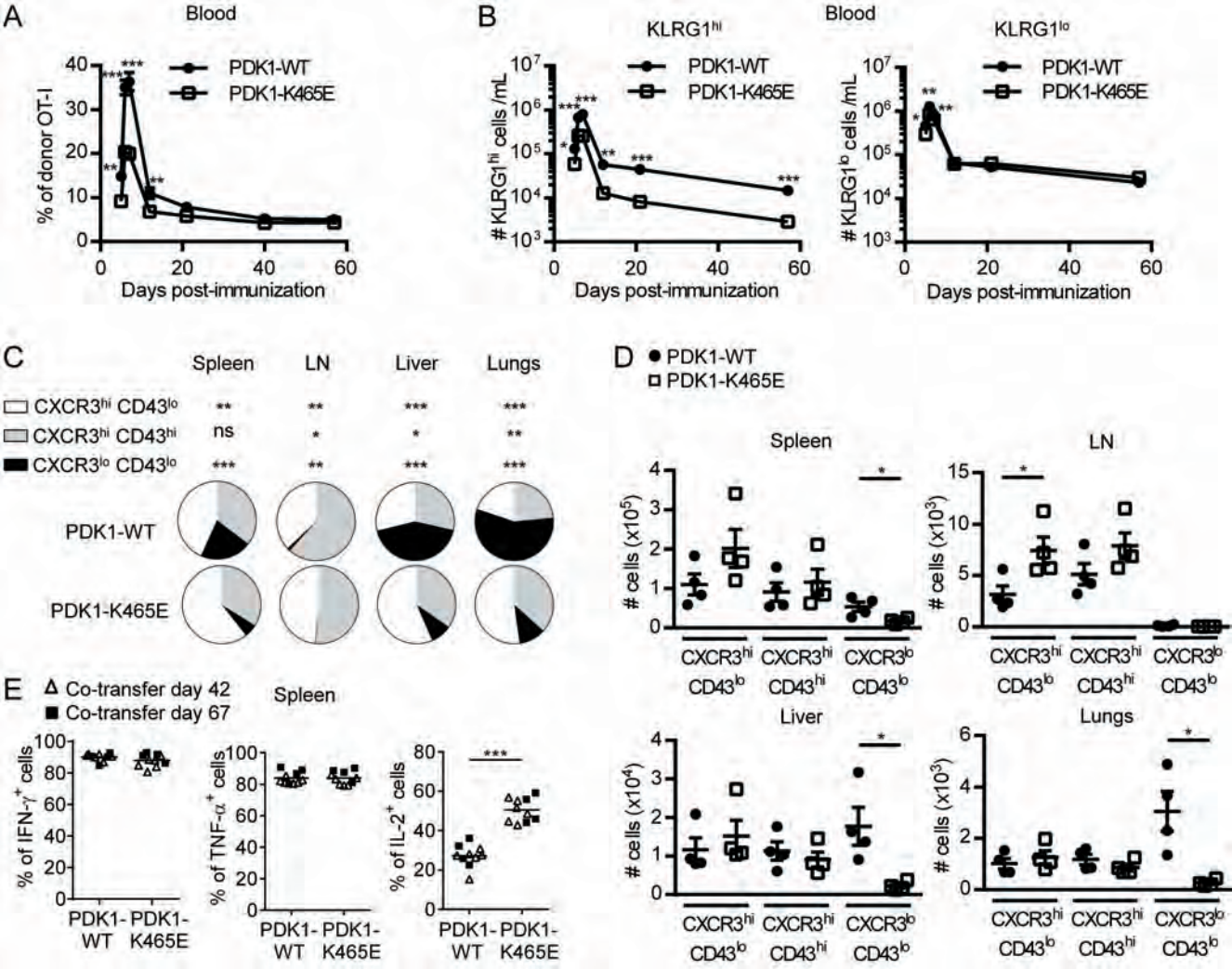
A
Blood
PDK1-WT
PDK1-K465E
% of donor OT-I
Days post-immunization
B
KLRG1hi
KLRG1lo
Blood
KLRG1hi cells /mL
KLRG1lo cells /mL
Days post-immunization
C
Spleen
LN
Liver
Lungs
CXCR3hi CD43lo
CXCR3hi CD43hi
CXCR3lo CD43lo
ns
PDK1-WT
PDK1-K465E
D
PDK1-WT
PDK1-K465E
Spleen
LN
Liver
Lungs
cells (x10^5)
cells (x10^3)
cells (x10^4)
CXCR3hi CD43lo
CXCR3hi CD43hi
CXCR3lo CD43lo
E
Co-transfer day 42
Co-transfer day 67
Spleen
% of IFN-γ+ cells
% of TNF-α+ cells
% of IL-2+ cells
PDK1-WT
PDK1-K465E

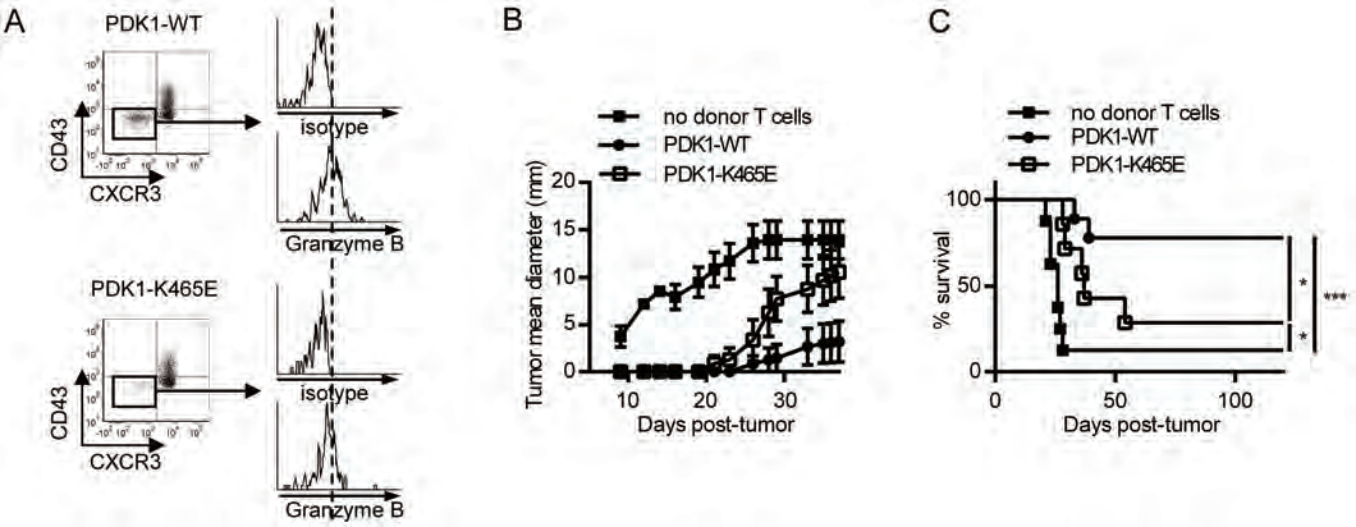
A
PDK1-WT
CD43
CXCR3
isotype
Granzyme B
PDK1-K465E
CD43
CXCR3
isotype
Granzyme B
B
no donor T cells
PDK1-WT
PDK1-K465E
Tumor mean diameter (mm)
20
15
10
5
0
10
20
30
Days post-tumor
C
no donor T cells
PDK1-WT
PDK1-K465E
% survival
100
50
0
0
50
100
Days post-tumor
*
*
***

Supporting Information

SI Materials and Methods

Flow cytometry

Antibodies against CD8α (53-6.7), CD45.1 (A20), CD45.2 (104), CD127 (A7R34), KLRG1 (2F1), CXCR3 (CXCR3-173), CD62L (MEL-14), Eomes (DAN11MAG), T-bet (eBio4B10), IFN-γ (XMG1.2), TNF-α (MP6-XT22), IL-2 (JES6-5H4) and CD107a (eBio1D4B) were purchased from ebioscience. Antibodies against CD43 (activation glycoform, 1B11), CD8β (YTS156.7.7) and CX_3CR1 (SA011F11) were purchased from Biolegend, anti-granzyme B (GB11) antibody from Life Technologies and anti-Ki67 (B56) from BD Biosciences. Intracellular staining for granzyme B, Eomes and T-bet was performed using the Foxp3 staining buffer kit (ebioscience). For intracellular staining of cytokines, splenocytes were stimulated with 10 pM or 1 nM of $OVA_{257-264}$ peptide (PeptideSynthetics) at 37ºC for 4 hours, in the presence of GolgiPlug (BD Biosciences). After culture, cells were stained for cell surface molecules and intracellular staining was performed using the BD Biosciences Cytofix/Cytoperm buffers.

Cell preparation for Western Blot analysis

For the analysis of Akt and S6 phosphorylation, PDK1-WT and PDK1-K465E OT-I splenocytes were stimulated with 10 pM $OVA_{257-264}$ for 2 days and then expanded in IL-2 (10 ng/mL) for 3 days. CTL (>95% $CD8^+$) were washed and rested for 30 minutes prior to restimulation with $OVA_{257-264}$ for 5, 10 or 15 minutes. Control PDK1-WT cells were treated with 1 μM of Akt1/2 inhibitor VIII (Merck Millipore) for the whole culture. For Bim analysis, splenocytes harvested from mice primed 7 days earlier with OVA/anti-CD40/LPS or ΔActA-

Lm-OVA were stained with a biotinylated anti-CD45.1 antibody. CD45.1 cells were isolated by immuno-magnetic selection using anti-biotin Microbeads (Miltenyi) before performing protein extraction.

Western Blot antibodies

Antibodies against phospho-S6 Ser235/236 (clone D57.2.2E), S6 ribosomal protein (clone 5G10), phospho-Akt Thr308 (clone 244F9) and Akt (polyclonal rabbit Ab) were purchased from Cell Signaling Technology. Anti-Bim antibody (clone 3C5) was purchased from Enzo Life Sciences, anti-actin antibody (clone C-11) and HRP-linked anti-goat antibody from Santa Cruz Biotechnology. HRP-linked anti-rabbit antibody was purchased from GE Healthcare Life Sciences.

Intravascular staining

Intravascular staining was performed as described by Anderson et al (19). Briefly, mice were injected i.v. with 3 µg of anti-CD8α APC-mAb (53-6.7, ebioscience), culled 3 minutes later, and lymphocytes were isolated, stained and analyzed by flow cytometry.

***In vitro* killing assay**

8 weeks after PDK1-WT or PDK1-K465E OT-I adoptive transfer and infection with ΔActA-Lm-OVA, splenocytes were harvested and stained with a biotinylated anti-CD45.1 antibody. CD45.1 PDK1-WT and PDK1-K465E memory cells were enriched by immuno-magnetic selection using anti-biotin Microbeads (Miltenyi). Targets cells were CD45.2 C57BL/6 naive splenocytes either loaded with 10 µM $OVA_{257-264}$ or left unpulsed for 1 hour at 37°C. Peptide-pulsed targets and unpulsed targets were stained for 10 minutes at 37°C with 1 µM CFSE and 0.1 µM CFSE, respectively. $CFSE^{high}$ and $CFSE^{lo}$ targets were mixed at a 1:1 ratio

and were incubated alone or with PDK1-WT or PDK1-K465E memory cells for 6h at 37°C, in triplicates. The ratios of the surviving $CFSE^{high}$ and $CFSE^{low}$ cell populations were assessed by flow cytometry. Specific killing was calculated as follows: % killing = 100*[1-($CFSE^{high}$ / $CFSE^{low}$)$_{effectors}$/($CFSE^{high}$ / $CFSE^{low}$)$_{control}$].

Tumor-infiltrating T cells analysis

When the humane endpoint was reached (15 mm mean tumor diameter), tumors and spleens were digested for 30 minutes at 37ºC using 50 µg/mL DNAse I (Roche) and 0.52 Wünsch Unit/mL of liberase DL (Roche) and mashed through a 100 µm cell strainer before staining for flow cytometry analysis.

SI Figure legends

Fig. S1, related to Figure 1. *(A,B)* PDK1-WT and PDK1-K465E OT-I splenocytes were stimulated for 2 days with $OVA_{257-264}$ and cultured in IL-2 for 3 additional days, prior to restimulation with $OVA_{257-264}$ for 5, 10 or 15 minutes. Control PDK1-WT cells were treated with the Akt1/2 inhibitor for the whole culture. Data show *(A)* levels of Akt phosphorylation at Thr308 and *(B)* levels of S6 ribosomal subunit phosphorylation at Ser235/236. *(C,D,E,G)* 10^4 or *(F,H)* 10^5 CD45.1 PDK1-WT or PDK1-K465E OT-I cells were adoptively transferred to CD45.2 C57BL/6 recipient mice followed by vaccination with *(C,D)* OVA/anti-CD40 mAb/LPS, *(E,G)* OVA/anti-4-1BB mAb/LPS or *(F,H)* OVA/polyI:C. Spleens were harvested *(C,D,E,G)* on day 6 or *(F,H)* on day 5 post-priming. *(C)* Representative dot plots of IFN-γ, TNF-α and IL-2 intracellular staining and *(D)* IFN-γ, TNF-α and IL-2 MFI of cytokine-expressing PDK1-WT and PDK1-K465E cells following *ex vivo* re-stimulation of splenocytes with 10 pM or 1 nM of $OVA_{257-264}$. *(E,F)* Frequency of granzyme B^+ cells among

PDK1-WT and PDK1-K465E OT-I cells in spleen and *(G,H)* frequency of PDK1-WT and PDK1-K465E cells producing IFN-γ, TNF-α or IL-2 following *ex vivo* re-stimulation of splenocytes with 1 nM of $OVA_{257-264}$ after priming with *(E,G)* OVA/anti-4-1BB/LPS or *(F,H)* OVA/polyI:C. Data show the mean ± SEM of *(D,F)* two combined experiments with n=4 mice/group/experiment or *(E,G,H)* one experiment with n=3-4 mice/group. *p≤ 0.05, **p≤ 0.01.

Fig. S2, related to Figure 2. Following adoptive transfer of CD45.1 PDK1-WT or PDK1-K465E OT-I cells, recipient mice were vaccinated with OVA/anti-CD40/LPS and spleen, inguinal LNs, blood, liver, lungs and colon were harvested 6-7 weeks later. *(A,B,E)* Mice were injected i.v. with anti-CD8α APC-mAb, culled 3 min later and lymphocytes were isolated, stained and analyzed by flow cytometry. *(A)* Representative dot plots of intravascular staining with anti-CD8α mAb, gated on $CD8\beta^+$ CD45.1 PDK1-WT cells. Numbers in dot plots indicate the proportion of cells stained with the anti-CD8α mAb (LP; lamina propria). *(B)* Frequency of PDK1-WT and PDK1-K465E OT-I in the $CD8\beta^+$ CD8α mAb i.v.+ and the $CD8\beta^+$ CD8α mAb i.v.- fractions in lungs, liver and colon LP, with each data point representing an individual mouse. N.D.; not detected. *(C)* Frequency of $CD62L^{hi}$ cells among PDK1-WT and PDK1-K465E donor OT-I. *(D)* Expression of CD62L, KLRG-1 and granzyme B by PDK1-WT $CXCR3^{hi}CD43^{lo}$, $CXCR3^{hi}CD43^{hi}$ and $CXCR3^{lo}CD43^{lo}$ memory cells in spleen. Dotted lines are set against matching isotypes. *(E)* Representative histogram overlays of CXCR3 (upper panel) and KLRG1 (bottom panel) expression on PDK1-WT cells stained with anti-CD8α mAb i.v (black line) or protected from i.v. staining (shaded histogram). Data show the mean ± SEM of *(B)* one experiment with n=3 mice/group, with each data point representing an individual mouse and *(C)* two combined

experiments with n=3 mice/group/experiment. *(A,D,E)* Data are from one representative experiment. *p≤ 0.05, ***p≤ 0.001.

Fig. S3, related to Figure 3. *(A)* Mice received a 1:1 ratio co-transfer of PDK1-WT and PDK1-K465E OT-I cells followed by OVA/anti-CD40/LPS vaccine and were re-challenged at the memory phase with $OVA_{257-264}$. Data show the frequency of granzyme B^+ cells in blood among PDK1-WT and PDK1-K465E OT-I cells on day 4 and day 7 after re-challenge. *(B)* Adoptive transfer of 10^4 PDK1-WT and PDK1-K465E OT-I, vaccination with OVA/anti-CD40/LPS and re-challenge with $OVA_{257-264}$ were performed as in Fig. 3. Data show the numbers of CD45.1 Tetramer $^+$ OT-I cells per mL of blood prior to and 4 days (left panel) or 7 days (right panel) after re-challenge, with each symbol representing an individual mouse. Mean fold expansion ± SEM is given. Data are from one experiment representative of three. *(C,D)* Mice received *(C)* 10^5 or *(D)* 10^4 PDK1-WT or PDK1-K465E OT-I cells followed by vaccination with *(C)* OVA/polyI:C or *(D)* OVA/anti-4-1BB/LPS and then were re-challenged (indicated by the arrow) at the memory phase with $OVA_{257-264}$/anti-CD40 mAb. Data show the mean ± SEM of the frequency of donor OT-I cells among $CD8^+$ T cells in blood and are representative of *(C)* two experiments with n=3-4 mice/group/experiment and *(D)* one experiment with n=4 mice/group. *p≤ 0.05, **p≤ 0.01, ***p≤ 0.001.

Fig. S4, related to Figure 4. Following adoptive transfer of PDK1-WT or PDK1-K465E OT-I cells, recipient mice were vaccinated with OVA/anti-CD40 mAb/LPS. Spleens were harvested 6 days later and CD127 expression on $KLRG1^{hi}$ and $KLRG1^{lo}$ PDK1-WT and PDK1-K465E OT-I cells was assessed. Data show the mean ± SEM of two combined experiments with n=4 mice/group/experiment. **p≤ 0.01, ***p≤ 0.001.

Fig. S5, related to Figure 5. Single transfer (filled symbols) or co-transfer (open symbols) of PDK1-WT and PDK1-K465E OT-I cells and infection with ΔActA-Lm-OVA were

performed as in Fig. 5. Spleens and blood samples were harvested on day 6 post-infection. *(A)* Frequency of $Ki67^+$ cells among donor PDK1-WT and PDK1-K465E OT-I in spleen following co-transfer. *(B)* Representative dot plot of CD127 and KLRG-1 expression on PDK1-WT and PDK1-K465E donor OT-I in blood. *(C)* CD127 expression on $KLRG\text{-}1^{hi}$ and $KLRG\text{-}1^{lo}$ PDK1-WT and PDK1-K465E OT-I cells in spleen. *(D)* Frequency of $KLRG\text{-}1^{hi}$ cells among donor PDK1-WT and PDK1-K465E OT-I in blood. *(E)* Frequency of granzyme B^+ cells among donor PDK1-WT and PDK1-K465E OT-I. Right panel shows representative histogram overlays of the expression of granzyme B in PDK1-WT (shaded histograms) and PDK1-K465E OT-I cells (black line). Dotted lines show the corresponding isotypes. *(F)* Frequency of $CD107a^+$ cells among donor PDK1-WT and PDK1-K465E OT-I cells following *ex vivo* re-stimulation with 1 nM of $OVA_{257\text{-}264}$. *(G,H,I)* Splenocytes were re-stimulated *ex vivo* with 10 pM or 1 nM of $OVA_{257\text{-}264}$. Data show *(G)* the frequency of CD45.1 PDK1-WT and PDK1-K465E OT-I producing IFN-γ or TNF-α, *(H)* representative dot plots of IFN-γ, TNF-α and IL-2 intracellular staining and *(I)* IFN-γ, TNF-α and IL-2 MFI of cytokine-expressing PDK1-WT and PDK1-K465E cells. Data show *(A)* one representative experiment of two with n=3-5 mice/experiment, *(C,D,I)* the mean ± SEM of one experiment representative of two (one single transfer with n=4 mice/group and one co-transfer with n=5 mice), *(E,G)* the mean of two combined experiments (one single transfer with n=4 mice/group and one co-transfer with n=5 mice) with each symbol representing an individual mouse, and *(F)* the mean ± SEM of one experiment with n=4 mice/group. *p≤ 0.05, ***p≤ 0.001.

Fig. S6, related to Figure 6. Co-transfer of PDK1-WT and PDK1-K465E OT-I was performed as described in Fig. 5, mice were challenged with ΔActA-Lm-OVA and spleens, blood samples, inguinal LNs, livers and lungs were harvested 6-9 weeks later. *(A)* PDK1-WT:PDK1-K465E OT-I memory cell ratios and *(B)* numbers of $KLRG1^{hi}$ PDK1-WT and

PDK1-K465E OT-I cells in the different tissues. Data show *(A)* the mean of two combined experiments with n=4-6 mice/experiment and *(B)* the mean ± SEM of one experiment representative of two with n=4-6 mice/experiment, with each data point representing an individual mouse. *p≤ 0.05, **p≤ 0.01, ***p≤ 0.001.

Fig. S7, related to Figure 6. Co-transfer of PDK1-WT and PDK1-K465E OT-I cells and infection with ΔActA-Lm-OVA were performed as in Fig. 5. Fifty three days post-infection, mice were injected i.v. with anti-CD8α APC-mAb, culled 3 min later, and spleen, inguinal lymph nodes, blood, liver and lungs were harvested. Lymphocytes were isolated, stained and analyzed by flow cytometry. *(A)* Representative dot plots of intravascular staining with anti-CD8α mAb, gated on CD8β$^+$ CD45.1 PDK1-WT or PDK1-K465E OT-I cells. Numbers in dot plots indicate the proportion of cells stained with the anti-CD8α mAb. *(B,C)* Representative histogram overlays of *(B)* CXCR3 and *(C)* KLRG1 expression on PDK1-WT and PDK1-K465E cells stained with anti-CD8α mAb i.v (black line) or protected from the i.v. staining (shaded histogram). *(D)* PDK1-WT:PDK1-K465E OT-I memory cell ratios in the CD8α mAb iv+ or iv- fractions, with each data point representing an individual mouse. Data are from one experiment with n=4 mice. **p≤ 0.01.

Fig. S8, related to Figures 6 and 7. Co-transfer of PDK1-WT and PDK1-K465E OT-I was performed as described in Fig. 5. Mice were infected with ΔActA-Lm-OVA and spleens were harvested 6-9 weeks post-infection. *(A,B)* Splenocytes were re-stimulated *ex vivo* with 1 nM of $OVA_{257-264}$. Data show *(A)* representative dot plots of IFN-γ, TNF-α and IL-2 intracellular staining and *(B)* pie charts depicting the frequency of PDK1-WT and PDK1-K465E OT-I in spleen producing IFN-γ only, IFN-γ and TNF-α or IFN-γ, TNF-α and IL-2. *(C)* Expression of granzyme B in PDK1-WT and PDK1-K465E memory subsets was analyzed directly *ex vivo*. *(D)* Cytotoxicity of PDK1-WT and PDK1-K465E memory cells against $OVA_{257-264}$-pulsed

targets. Data are from *(B)* two combined experiments with n=4-6 mice/experiment, *(C)* one experiment representative of two with n= 4 mice/experiment and *(D)* one experiment with n=3-4 mice/group. **p≤ 0.01, ***p≤ 0.001.

Fig. S9, related to Figure 7. Single transfer of PDK1-WT and PDK1-K465E OT-I cells and infection of recipient mice with ΔActA-Lm-OVA were performed as in Fig. 5. On day 48 post-infection, mice were challenged, without further boosting, with $5x10^5$ E.G7 tumor cells (s.c.). When the humane endpoint was reached, tumors and spleens were harvested. *(A)* Frequency of CD45.1 PDK1-WT and PDK1-K465E cells among tumor-infiltrating $CD8^+$ T cells. *(B)* Representative dot plots of CXCR3 and CD43 expression gated on PDK1-WT and PDK1-K465E cells in spleen and tumor. *(C)* Expression of CX_3CR1 on PDK1-WT memory subsets in spleen. *(D)* Representative dot plots of CX_3CR1 expression on PDK1-WT and PDK1-K465E cells in tumors. *(E)* Frequency of PDK1-WT and PDK1-K465E cells expressing CX_3CR1 in tumors, with each symbol representing an individual mouse. Data are from one experiment with n=3-6 mice/group. *p≤ 0.05.

Fig. S10. Single transfer of PDK1-WT and PDK1-K465E OT-I cells and infection with ΔActA-Lm-OVA were performed as in Fig. 5. On day 7 post-infection, Bim and actin expression levels in purified splenic PDK1-WT and PDK1-K465E OT-I cells were analyzed by Western blotting and densitometry. Bar graphs represent the ratio of Bim to actin expressed as % of PDK1-WT values. Data show the mean ± SEM of 2 combined experiments with n=3-4 mice/group.

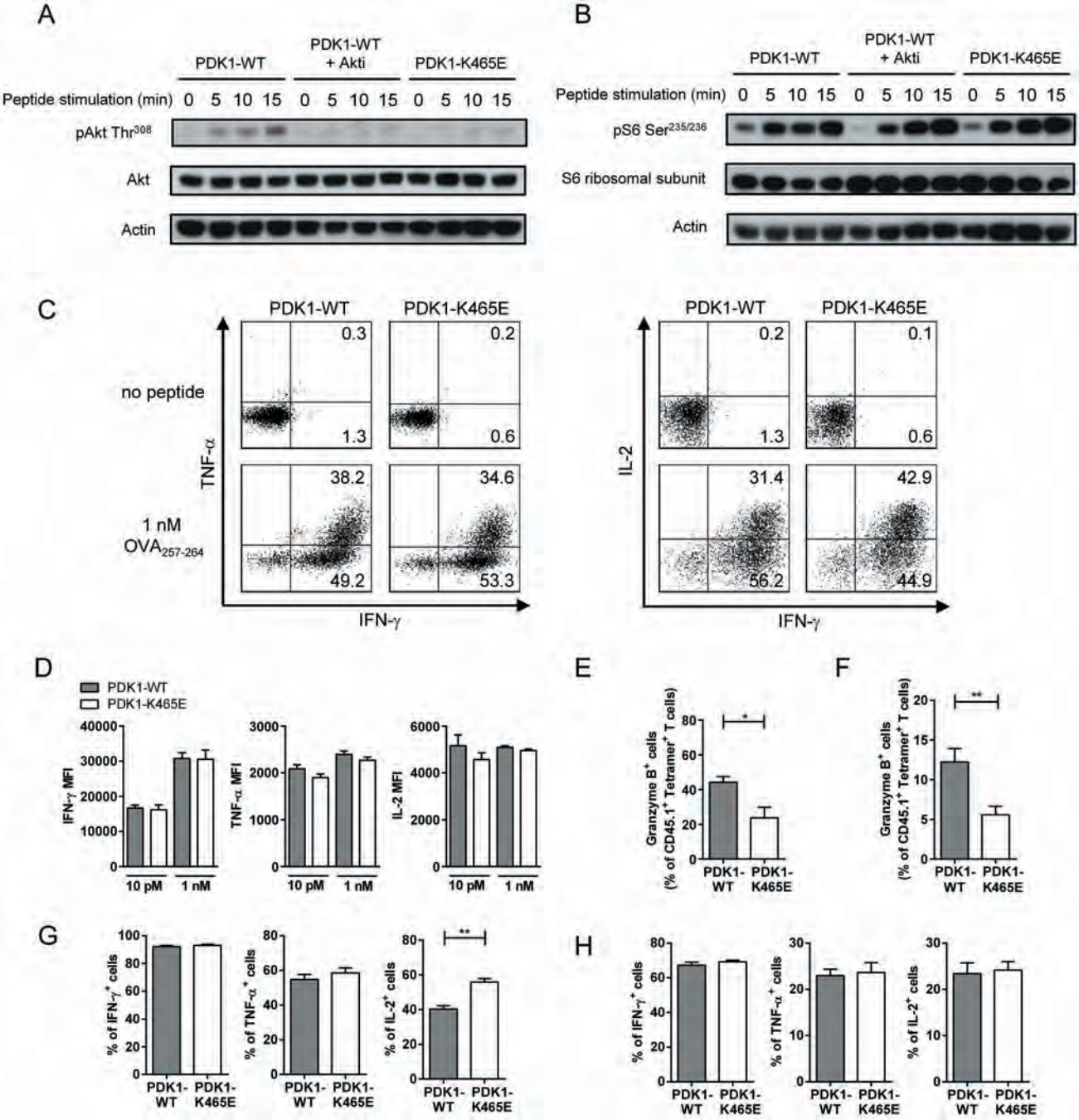
A
PDK1-WT
PDK1-WT + Akti
PDK1-K465E
Peptide stimulation (min) 0 5 10 15 0 5 10 15 0 5 10 15
pAkt Thr308
Akt
Actin
B
PDK1-WT
PDK1-WT + Akti
PDK1-K465E
Peptide stimulation (min) 0 5 10 15 0 5 10 15 0 5 10 15
pS6 Ser235/236
S6 ribosomal subunit
Actin
C
PDK1-WT
PDK1-K465E
no peptide
1 nM OVA257-264
TNF-α
IFN-γ
0.3
0.2
1.3
0.6
38.2
34.6
49.2
53.3
IL-2
0.2
0.1
1.3
0.6
31.4
42.9
56.2
44.9
D
PDK1-WT
PDK1-K465E
IFN-γ MFI
TNF-α MFI
IL-2 MFI
10 pM
1 nM
E
Granzyme B+ cells (% of CD45.1+ Tetramer+ T cells)
PDK1-WT
PDK1-K465E
F
Granzyme B+ cells (% of CD45.1+ Tetramer+ T cells)
G
% of IFN-γ+ cells
% of TNF-α+ cells
% of IL-2+ cells
H
% of IFN-γ+ cells
% of TNF-α+ cells
% of IL-2+ cells

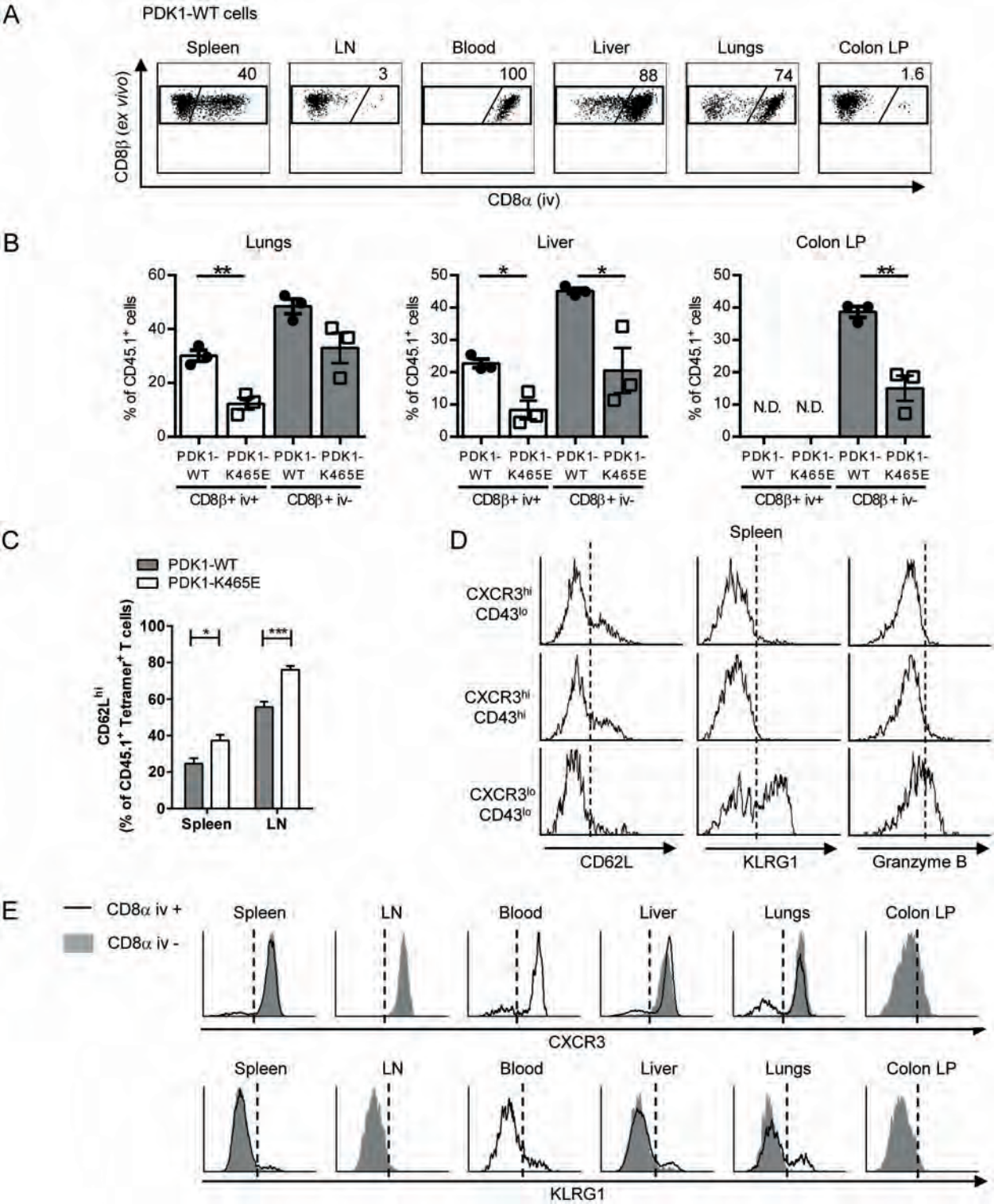
A
PDK1-WT cells
Spleen
LN
Blood
Liver
Lungs
Colon LP
40
3
100
88
74
1.6
CD8β (ex vivo)
CD8α (iv)
B
Lungs
Liver
Colon LP
% of CD45.1+ cells
N.D.
N.D.
PDK1-WT
PDK1-K465E
CD8β+ iv+
CD8β+ iv-
C
PDK1-WT
PDK1-K465E
CD62Lhi (% of CD45.1+ Tetramer+ T cells)
Spleen
LN
D
Spleen
CXCR3hi CD43lo
CXCR3hi CD43hi
CXCR3lo CD43lo
CD62L
KLRG1
Granzyme B
E
CD8α iv +
CD8α iv -
Spleen
LN
Blood
Liver
Lungs
Colon LP
CXCR3
KLRG1

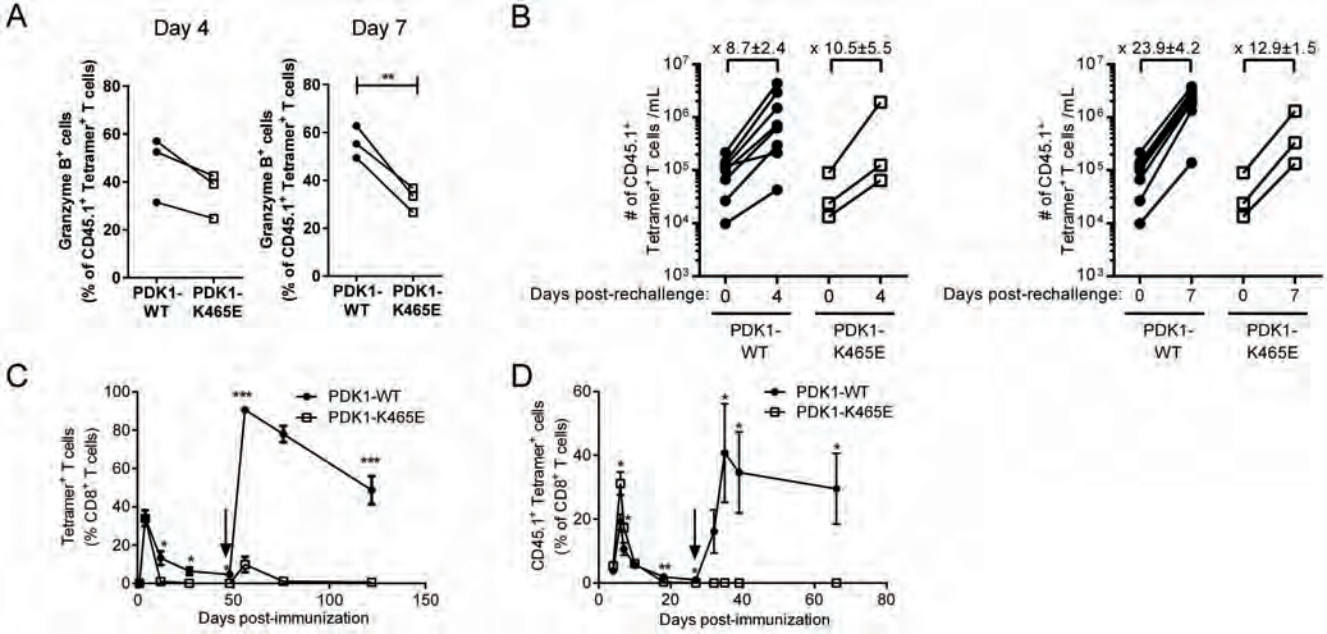
A
Day 4
Day 7
Granzyme B+ cells (% of CD45.1+ Tetramer+ T cells)
**
PDK1-WT
PDK1-K465E
B
x 8.7±2.4
x 10.5±5.5
x 23.9±4.2
x 12.9±1.5
# of CD45.1+ Tetramer+ T cells /mL
Days post-rechallenge: 0 4 0 4
Days post-rechallenge: 0 7 0 7
C
Tetramer+ T cells (% CD8+ T cells)
PDK1-WT
PDK1-K465E
Days post-immunization
D
CD45.1+ Tetramer+ cells (% of CD8+ T cells)
PDK1-WT
PDK1-K465E
Days post-immunization

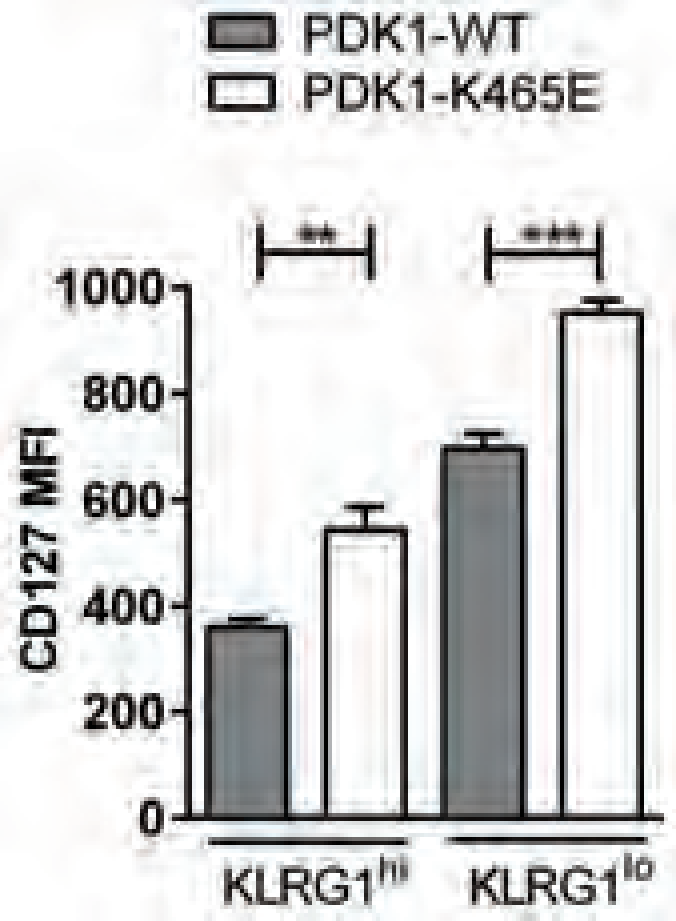
PDK1-WT
PDK1-K465E
**
***
1000
800
600
400
200
0
CD127 MFI
KLRG1hi
KLRG1lo

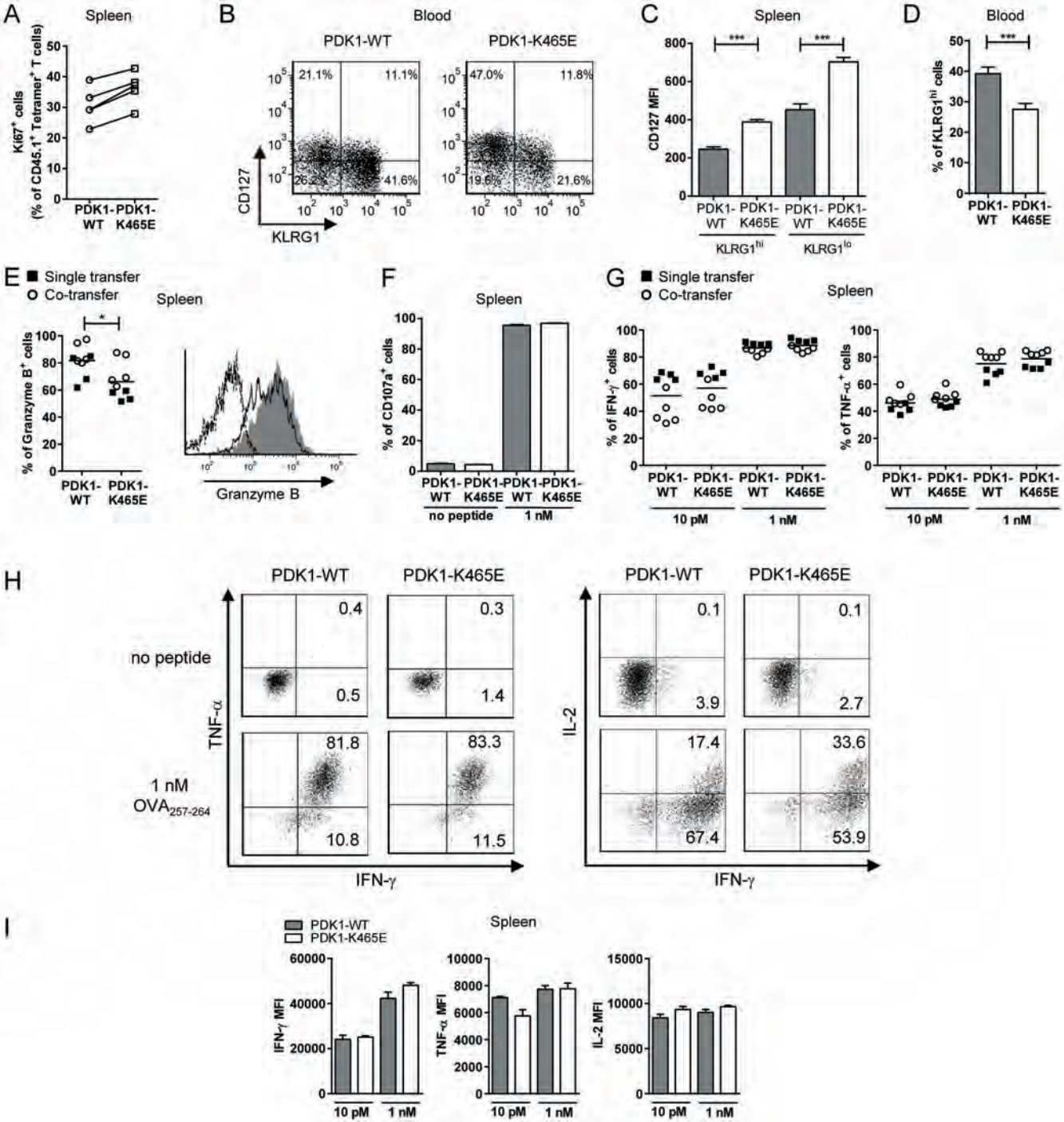
A
Spleen
Ki67+ cells (% of CD45.1+ Tetramer+ T cells)
PDK1-WT
PDK1-K465E
B
Blood
PDK1-WT
PDK1-K465E
21.1%
11.1%
26.2%
41.6%
47.0%
11.8%
19.6%
21.6%
CD127
KLRG1
C
Spleen
CD127 MFI
***
***
KLRG1hi
KLRG1lo
D
Blood
% of KLRG1hi cells
***
E
Single transfer
Co-transfer
Spleen
% of Granzyme B+ cells
*
Granzyme B
F
Spleen
% of CD107a+ cells
no peptide
1 nM
G
Single transfer
Co-transfer
Spleen
% of IFN-γ+ cells
% of TNF-α+ cells
10 pM
1 nM
H
PDK1-WT
PDK1-K465E
no peptide
1 nM OVA257-264
TNF-α
IFN-γ
0.4
0.3
0.5
1.4
81.8
83.3
10.8
11.5
IL-2
IFN-γ
0.1
0.1
3.9
2.7
17.4
33.6
67.4
53.9
I
PDK1-WT
PDK1-K465E
Spleen
IFN-γ MFI
TNF-α MFI
IL-2 MFI
10 pM
1 nM

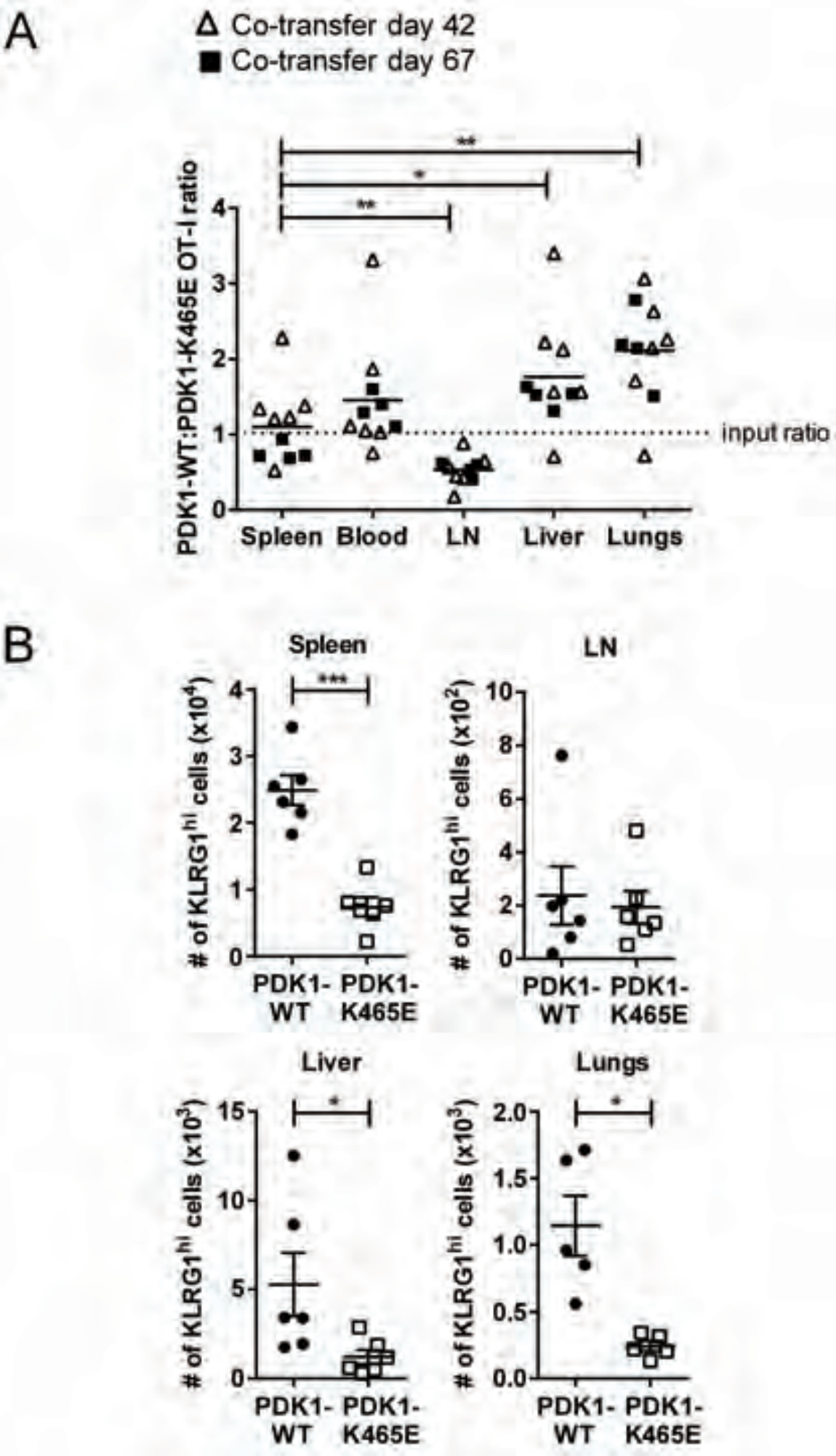
A
Co-transfer day 42
Co-transfer day 67
PDK1-WT:PDK1-K465E OT-I ratio
input ratio
Spleen
Blood
LN
Liver
Lungs
B
Spleen
LN
Liver
Lungs
# of KLRG1hi cells (x10^4)
# of KLRG1hi cells (x10^2)
# of KLRG1hi cells (x10^3)
PDK1-WT
PDK1-K465E

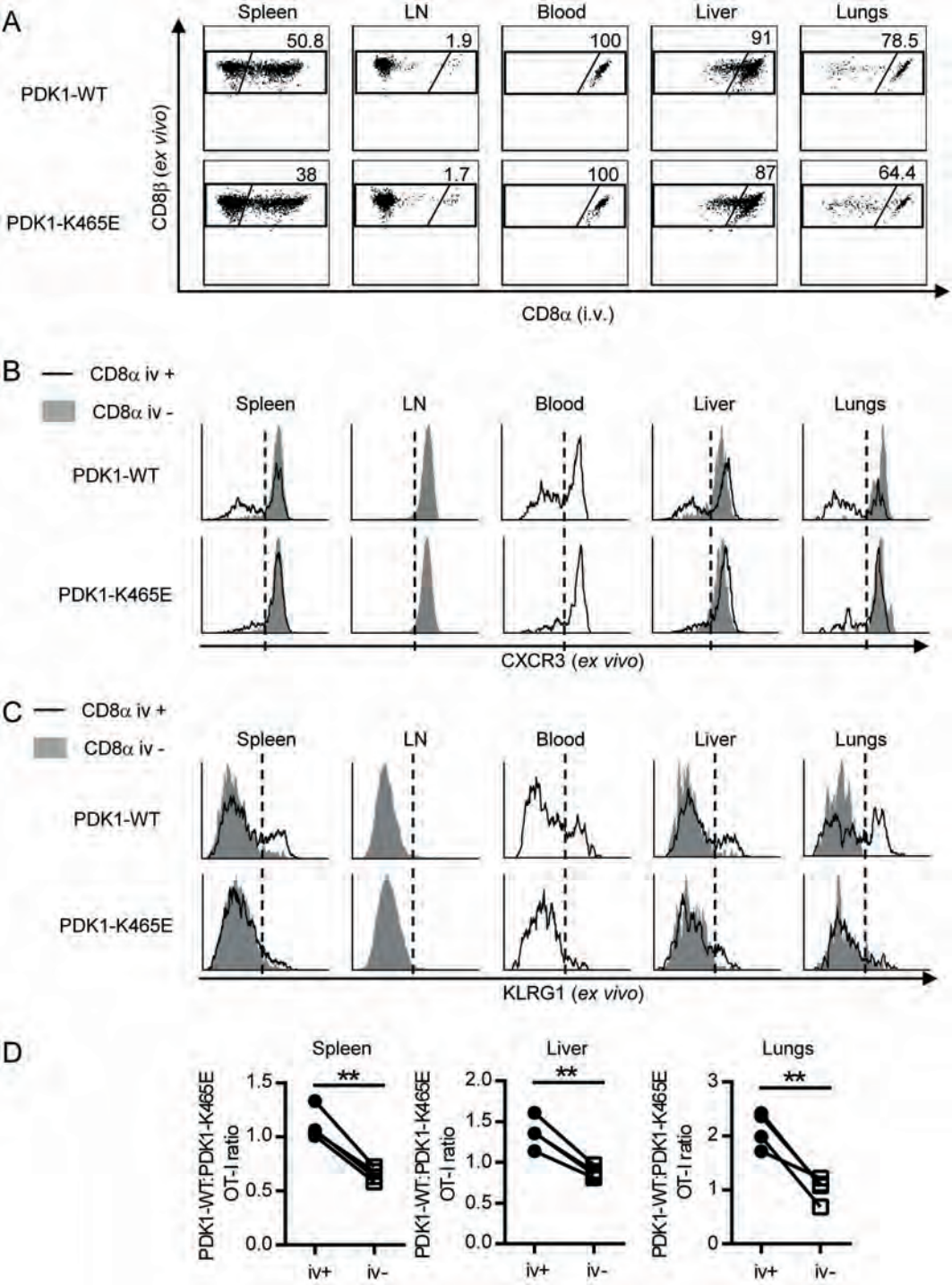
A
Spleen
LN
Blood
Liver
Lungs
PDK1-WT
PDK1-K465E
50.8
1.9
100
91
78.5
38
1.7
100
87
64.4
CD8β (ex vivo)
CD8α (i.v.)
B
CD8α iv +
CD8α iv -
Spleen
LN
Blood
Liver
Lungs
PDK1-WT
PDK1-K465E
CXCR3 (ex vivo)
C
CD8α iv +
CD8α iv -
Spleen
LN
Blood
Liver
Lungs
PDK1-WT
PDK1-K465E
KLRG1 (ex vivo)
D
Spleen
Liver
Lungs
PDK1-WT:PDK1-K465E OT-I ratio
**
1.5
1.0
0.5
0.0
2.0
3
2
1
0
iv+
iv-

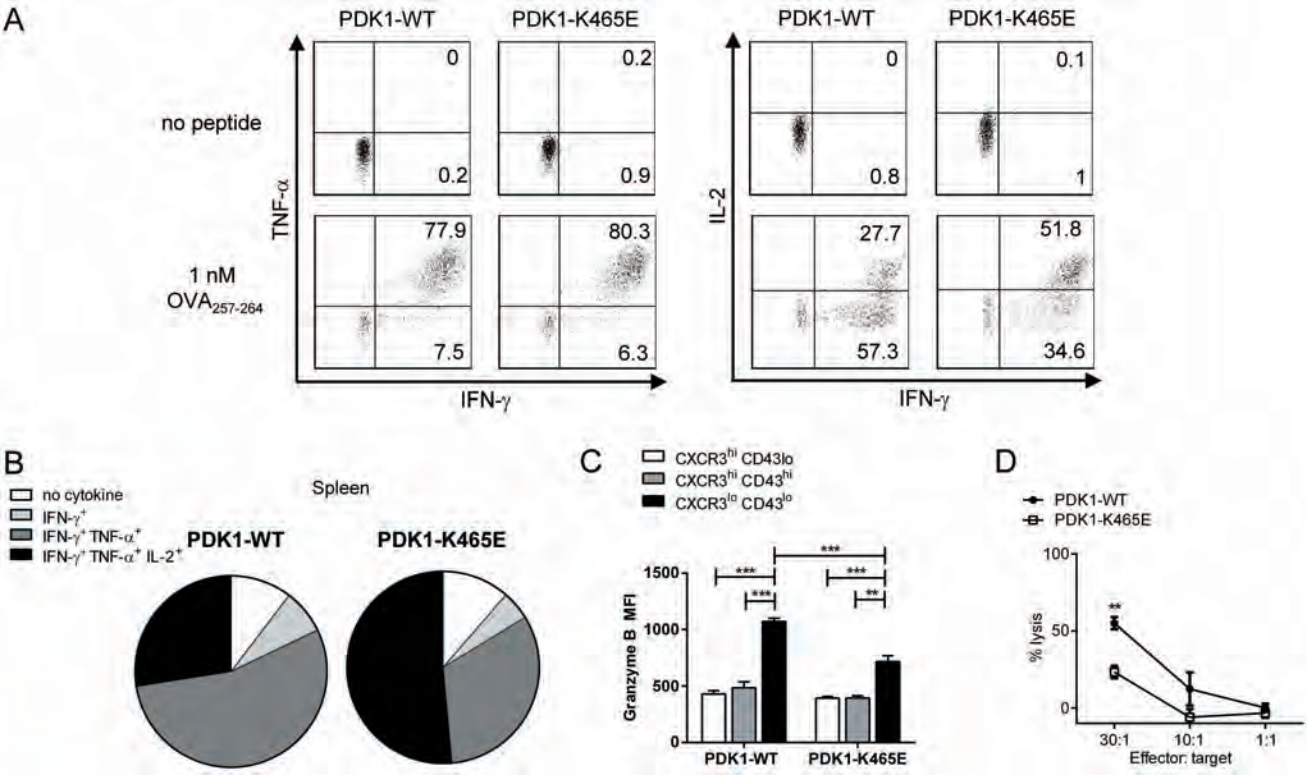
A
PDK1-WT
PDK1-K465E
PDK1-WT
PDK1-K465E
no peptide
1 nM OVA257-264
TNF-α
IFN-γ
IL-2
IFN-γ
0
0.2
0.2
0.9
77.9
7.5
80.3
6.3
0
0.8
0.1
1
27.7
57.3
51.8
34.6
B
Spleen
no cytokine
IFN-γ+
IFN-γ+ TNF-α+
IFN-γ+ TNF-α+ IL-2+
PDK1-WT
PDK1-K465E
C
CXCR3hi CD43lo
CXCR3hi CD43hi
CXCR3lo CD43lo
Granzyme B MFI
1500
1000
500
0
***
***
***
***
**
PDK1-WT
PDK1-K465E
D
PDK1-WT
PDK1-K465E
% lysis
100
50
0
**
30:1
10:1
1:1
Effector: target

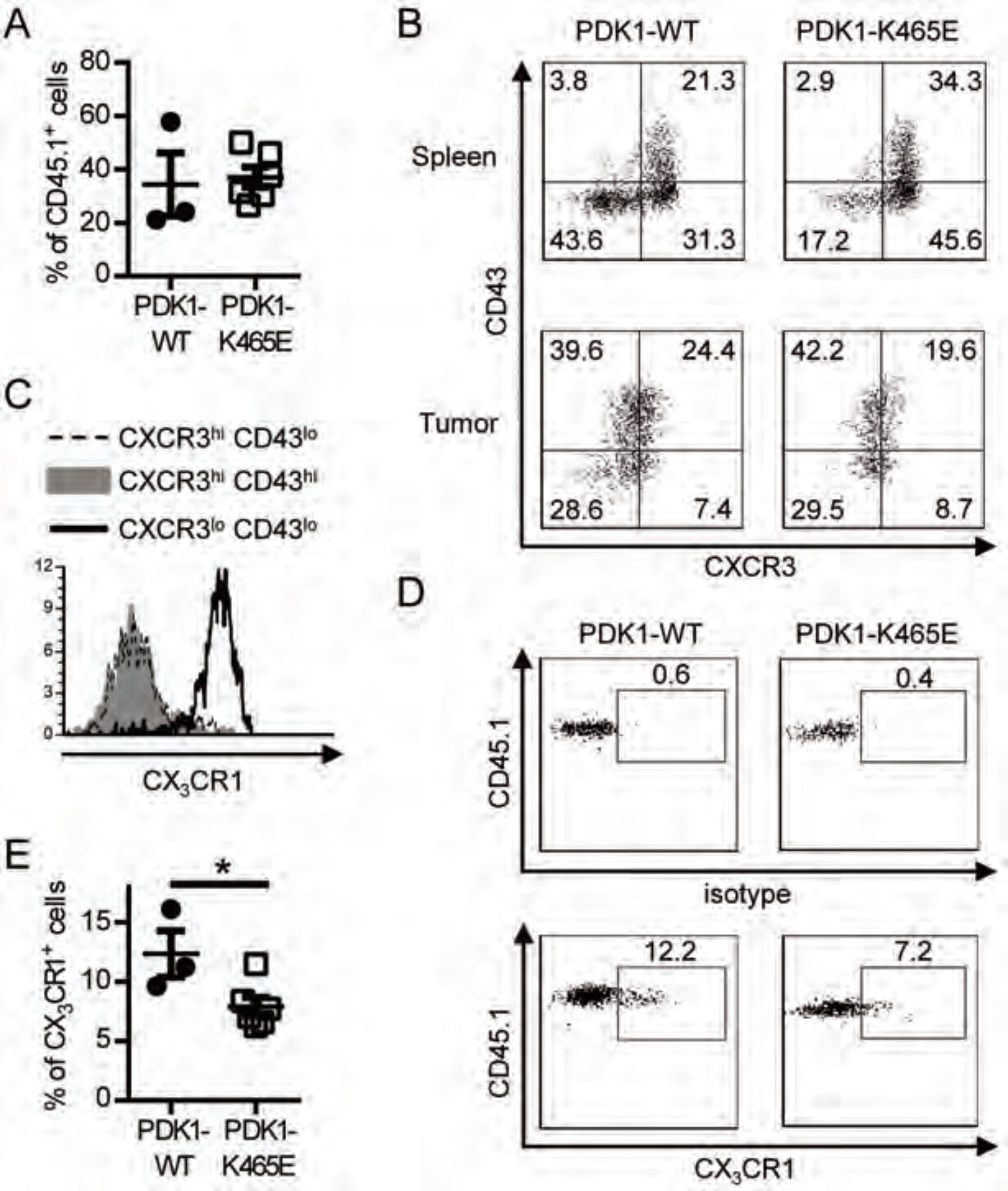
A
% of CD45.1+ cells
80
60
40
20
0
PDK1-WT
PDK1-K465E
B
PDK1-WT
PDK1-K465E
Spleen
Tumor
CD43
CXCR3
3.8
21.3
43.6
31.3
2.9
34.3
17.2
45.6
39.6
24.4
28.6
7.4
42.2
19.6
29.5
8.7
C
CXCR3hi CD43lo
CXCR3hi CD43hi
CXCR3lo CD43lo
CX3CR1
D
PDK1-WT
PDK1-K465E
CD45.1
isotype
0.6
0.4
12.2
7.2
CX3CR1
E
% of CX3CR1+ cells
*
15
10
5
0
PDK1-WT
PDK1-K465E

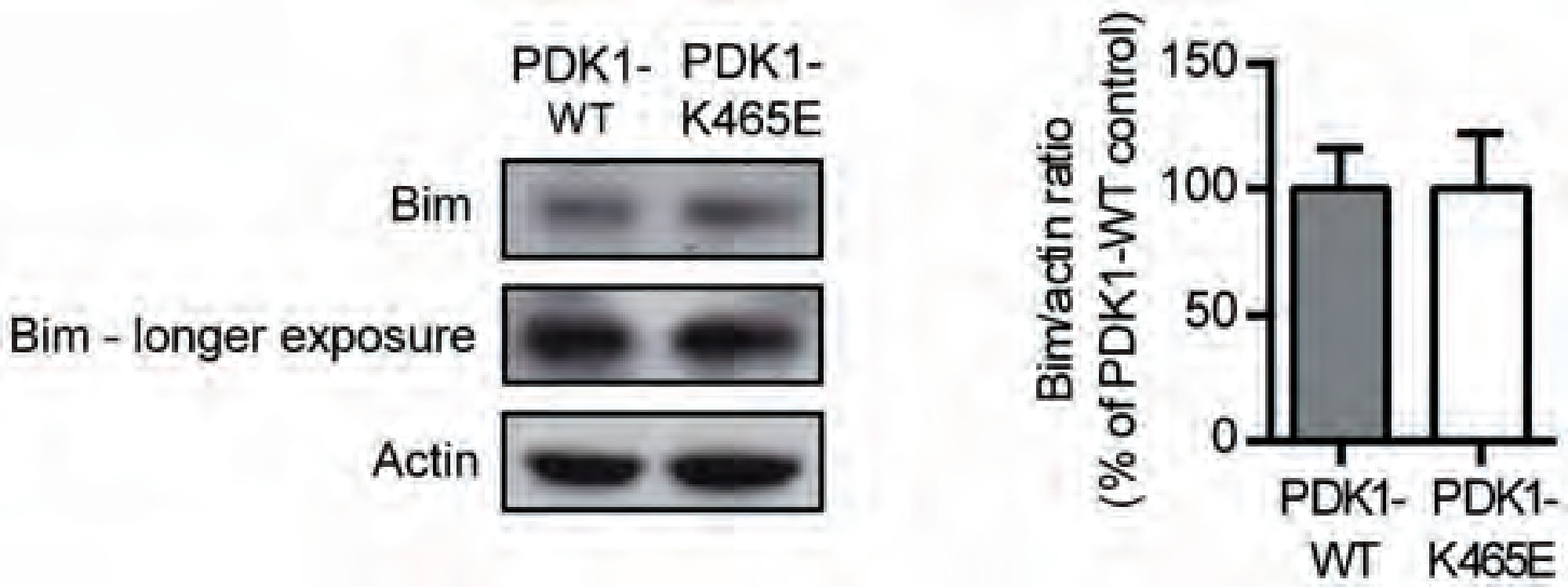
PDK1-
WT
PDK1-
K465E
Bim
Bim - longer exposure
Actin
Bim/actin ratio
(% of PDK1-WT control)
150
100
50
0
PDK1-
WT
PDK1-
K465E